Optimizing GC–MS Analysis of Explosives for Battlefield Forensics

ASMS 2020 Virtual Event Preview

On-Line SEC-MS Aggregate and Fragment Analysis of Therapeutic mAbs

Current Trends in MASS Spectrometry

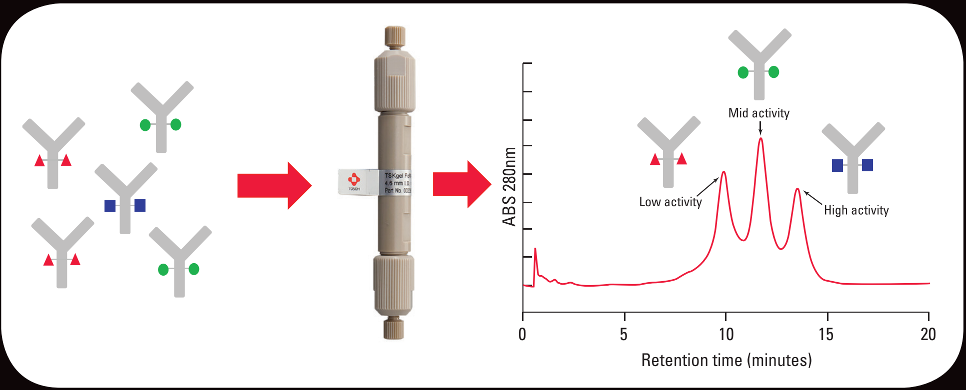

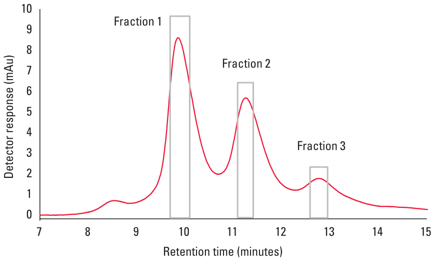

Detector response (mAu)
10
9
8
7
6
5
4
3
2
1
0
Fraction 1
Fraction 2
Fraction 3
7
8
9
10
11
12
13
14
15
Retention time (minutes)

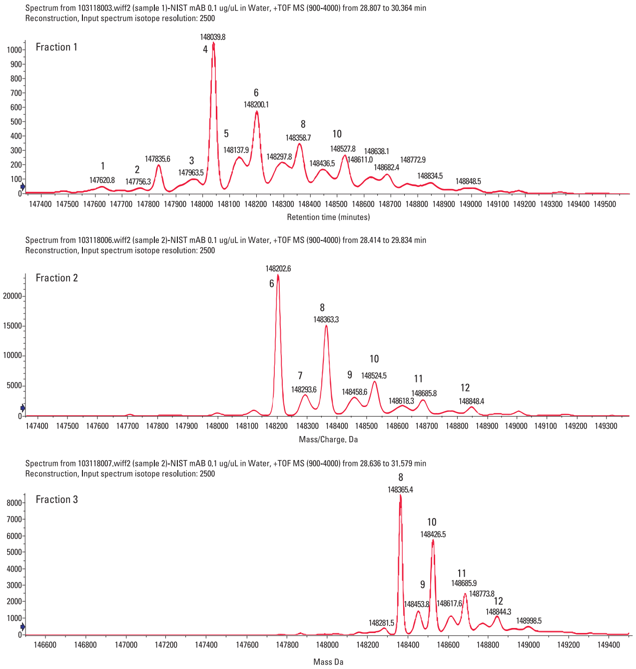

Spectrum from 103118003.wiff2 (sample 1)-NIST mAB 0.1 ug/uL in Water, +TOF MS (900-4000) from 28.807 to 30.364 min
Reconstruction, Input spectrum isotope resolution: 2500
Fraction 1
1000
900
800
700
600
500
400
300
200
100
0
148039.8
4
6
148200.1
5
148137.9
8
148358.7
10
148527.8
148638.1
148611.0
148682.4
148772.9
148834.5
148848.5
148297.8
148436.5
1
147620.8
2
147756.3
147835.6
3
147963.5
147400
147500
147600
147700
147800
147900
148000
148100
148200
148300
148400
148500
148600
148700
148800
148900
149000
149100
149200
149300
149400
149500
Retention time (minutes)
Spectrum from 103118006.wiff2 (sample 2)-NIST mAB 0.1 ug/uL in Water, +TOF MS (900-4000) from 28.414 to 29.834 min
Reconstruction, Input spectrum isotope resolution: 2500
Fraction 2
20000
15000
10000
5000
0
148202.6
6
8
148363.3
7
148293.6
9
148458.6
10
148524.5
148618.3
11
148685.8
12
148848.4
147400
147500
147600
147700
147800
147900
148000
148100
148200
148300
148400
148500
148600
148700
148800
148900
149000
149100
149200
149300
Mass/Charge. Da
Spectrum from 103118007.wiff2 (sample 2)-NIST mAB 0.1 ug/uL in Water, +TOF MS (900-4000) from 28.636 to 31.579 min
Reconstruction, Input spectrum isotope resolution: 2500
Fraction 3
8000
7000
6000
5000
4000
3000
2000
1000
0
8
148365.4
10
148426.5
9
148453.8
148617.6
11
148685.9
148773.8
12
148844.3
148998.5
148281.5
146600
146800
147000
147200
147400
147600
147800
148000
148200
148400
148600
148800
149000
149200
149400
Mass Da

Optimizing GC–MS Analysis of Explosives for Battlefield Forensics

ASMS 2020 Virtual Event Preview

On-Line SEC-MS Aggregate and Fragment Analysis of Therapeutic mAbs

Current Trends in MASS Spectrometry

Volume 18 Number 2 May 2020
www.chromatographyonline.com

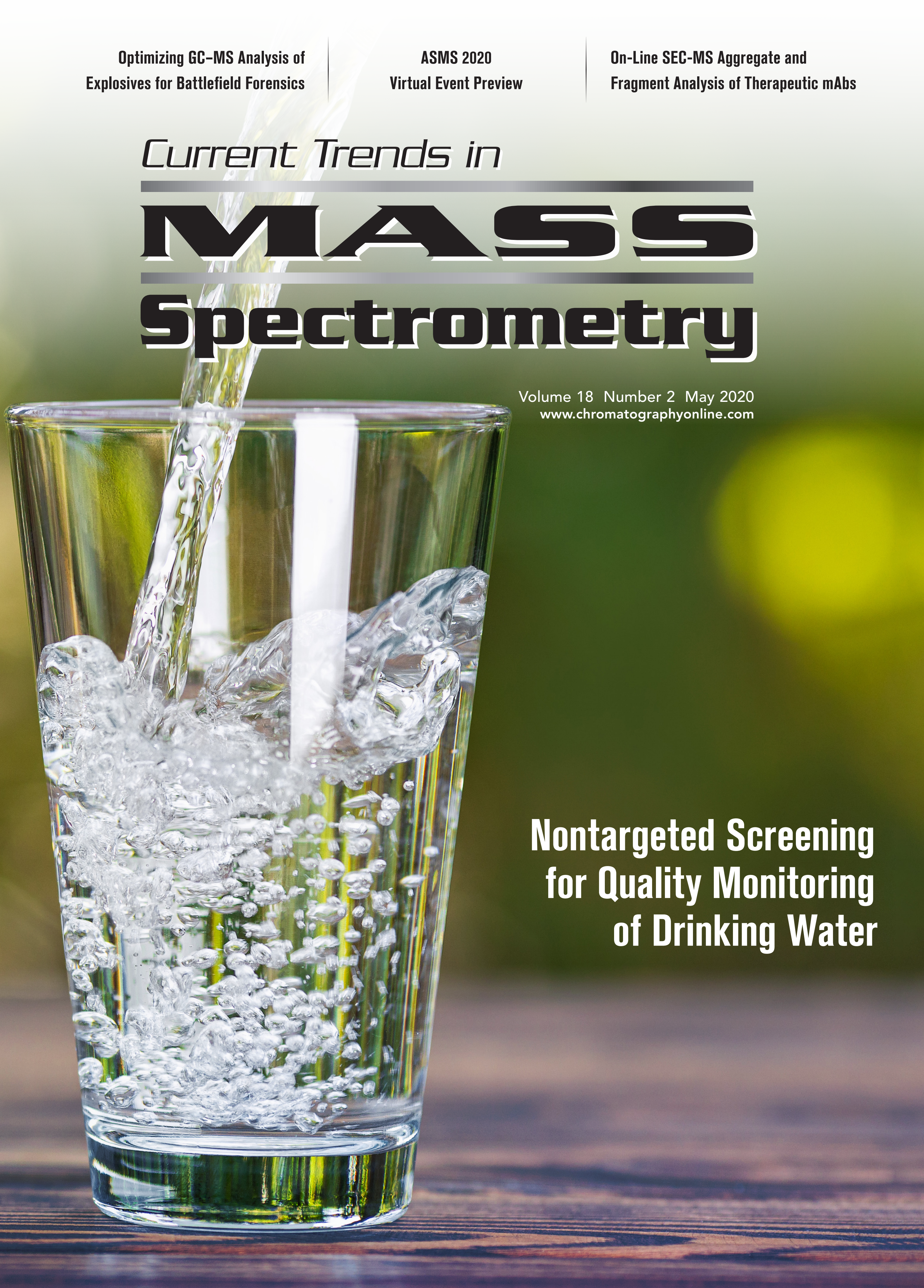

Nontargeted Screening for Quality Monitoring of Drinking Water

LCGC north america
solutions for separation scientists
LCGC europe
Spectroscopy

MANUSCRIPTS: For manuscript preparation guidelines, see chromatographyonline.com/lcgc-author-guidelines, or call The Editor, (732) 596-0276. LCGC welcomes unsolicited articles, manuscripts, photographs, illustrations, and other materials but cannot be held responsible for their safekeeping or return. Every precaution is taken to ensure accuracy, but LCGC cannot accept responsibility for the accuracy of information supplied herein or for any opinion expressed.

SUBSCRIPTIONS: For subscription and circulation information: LCGC, P.O. Box 457, Cranbury, NJ 08512-0457, or email mmhinfo@mmhgroup.com. Delivery of LCGC outside the United States is 14 days after printing. (LCGC Europe and LCGC Asia Pacific are available free of charge to users and specifiers of chromatographic equipment in Western Europe and Asia and Australia, respectively.)

CHANGE OF ADDRESS: Send change of address to LCGC, P.O. Box 457, Cranbury, NJ 08512-0457; alternately, send change via e-mail to fulfill@mjhassoc.com or go to the following URL: http://mmhpubs.mmhgroup.com/Welcome.aspx?pubid=LCGC Allow four to six weeks for change. PUBLICATIONS MAIL AGREEMENT No. 40612608. Return all undeliverable Canadian addresses to: IMEX Global Solutions, P.O. Box 25542, London, ON, N6C 6B2, CANADA. Canadian GST number: R-124213133RT001.

C.A.S.T. DATA AND LIST INFORMATION: Contact Melissa Stillwell, tel. (218) 740-6831, e-mail MStillwell@mmhgroup.com.

REPRINTS: Contact Michael J. Tessalone, e-mail: MTessalone@mmhgroup.com

INTERNATIONAL LICENSING: Contact Kim Scaffidi, e-mail: kscaffidi@mjhassoc.com

CUSTOMER INQUIRIES: Customer inquiries can be forwarded directly to MJH Life Sciences, Attn: Subscriptions, 2 Clarke Drive, Suite 100, Cranbury, NJ 08512; e-mail: mmhinfo@mmhgroup.com

Alliance for Audited Media

50% Recycled Paper 10-20% Post Consumer Waste

MultiMedia Pharma Sciences, LLC. provides certain customer contact data (such as customer's name, addresses, phone numbers, and e-mail addresses) to third parties who wish to promote relevant products, services, and other opportunities that may be of interest to you. If you do not want MultiMedia Pharma Sciences, LLC. to make your contact information available to third parties for marketing purposes, simply email mmhinfo@mmhgroup.com and a customer service representative will assist you in removing your name from MultiMedia Pharma Sciences, LLC. lists.

LCGC North America does not verify any claims or other information appearing in any of the advertisements contained in the publication, and cannot take responsibility for any losses or other damages incurred by readers in reliance of such content.

To subscribe, email mmhinfo@mmhgroup.com.

AN MJH life sciences™ BRAND

485F US Highway One South,
Suite 210
Iselin, NJ 08830
(732) 596-0276
Fax: (732) 647-1235

PUBLISHING/SALES

Group Vice President
Michael J. Tessalone
MTessalone@mjhlifesciences.com

Publisher
Stephanie Shaffer
SShaffer@mmhgroup.com

Associate Publisher
Edward Fantuzzi
EFantuzzi@mjhlifesciences.com

Sales Manager
Brianne Molnar
BMolnar@@mjhlifesciences.com

Account Executive
Timothy Edson
TEdson@mjhassoc.com

Senior Director, Digital Media
Michael Kushner
MKushner@mjhlifesciences.com

EDITORIAL

Editorial Director
Laura Bush
LBush@mjhlifesciences.com

Managing Editor
John Chasse
JChasse@mjhlifesciences.com

Senior Technical Editor
Jerome Workman
JWorkman@mjhlifesciences.com

Associate Editor
Cindy Delonas
CDelonas@mjhlifesciences.com

Creative Director, Publishing
Melissa Feinen
mfeinen@mdmag.com

Senior Art Director
Gwendolyn Salas
gsalas@mjhlifesciences.com

Graphic Designer
Courtney Soden
csoden@mjhlifesciences.com

CONTENT MARKETING

Custom Content Writer
Allissa Marrapodi
AMarrapodi@mjhlifesciences.com

Webcast Operations Manager
Kristen Moore
KMoore@mjhlifesciences.com

Project Manager
Vania Oliveira
VOliveira@mmhgroup.com

Digital Production Manager
Sabina Advani
SAdvani@mjhlifesciences.com

Managing Editor, Special Projects
Kaylynn Chiarello-Ebner
KEbner@mjhlifesciences.com

MARKETING/OPERATIONS

Marketing Manager
Brianne Pangaro
BPangaro@mjhlifesciences.com

C.A.S.T. Data and List Information
Melissa Stillwell
MStillwell@mmhgroup.com

Reprints
Alexandra Rockenstein
ARockenstein@mjhlifesciences.com

Audience Development Manager
Jessica Stariha
JStariha@mmhgroup.com

CORPORATE

Chairman & Founder
Mike Hennessy Sr

Vice Chairman
Jack Lepping

President & CEO
Mike Hennessy Jr

Chief Financial Officer
Neil Glasser, CPA/CFE

Executive Vice President, Global Medical Affairs & Corporate Development
Joe Petroziello

Executive Vice President, Operations
Tom Tolvé

Senior Vice President, Content
Silas Inman

Senior Vice President, I.T. & Enterprise Systems
John Moricone

Senior Vice President, Audience Generation & Product Fulfillment
Joy Puzzo

Vice President, Human Resources & Administration
Shari Lundenberg

Vice President, Business Intelligence
Chris Hennessy

Executive Creative Director, Creative Services
Jeff Brown

Current Trends in
MASS
Spectrometry

May 2020

Articles

Departments

Cover image courtesy of alter_photo/stock.adobe.com

Nontargeted Screening as an Essential Tool for Drinking Water Quality Monitoring

The treatment of water for human use and consumption can lead to the generation of potentially hazardous transformation products (TPs) from organic micropollutants (OMPs), a group of synthetic chemicals present in water sources at very low concentrations. Despite the potential toxicity of TPs, they are not measured routinely, due to the analytical challenges associated with their identification. One of the major challenges is confidently identifying OMPs and their TPs given the plethora of possible compounds known to exist. With advances in analytical methodology, a combination of targeted and nontargeted screening can be applied to identify the "known," "known unknown," and "unknown unknown" contaminants present within a sample. In this article, we present a study performed using liquid chromatography coupled with high-resolution mass spectrometry (LC–HRMS), in combination with a comprehensive data analysis workflow, to screen water samples for TPs to determine the efficacy of different water treatment methods.

Andrea Mizzi Brunner

Organic micropollutants (OMPs) are synthetic chemicals found in water sources and treated water at microgram-per-liter concentrations, or below (1). These persistent contaminants may be hazardous in themselves, and can also give rise to a wide variety of transformation products (TPs) (2,3,4). Potentially hazardous TPs may be formed from OMPs during drinking water treatment, but are not routinely measured, because of the lack of standards and significant analytical challenges involved in their identification. Ascertaining what TPs are removed or created during drinking water treatment is important for public health, as is determining their identity and toxicity. Advanced analytical methods based on liquid chromatography coupled with high- resolution mass spectrometry (LC–HRMS) are now being applied to aid in monitoring drinking water treatment steps, and to support a better understanding of these compounds.

A major issue in measuring OMPs and their TPs is the large number of possible compounds that can exist. OMPs and TPs can be considered as "knowns," "known unknowns," or "unknown unknowns." "Knowns" are, for example, those regulated priority pollutants that are actively screened for and which can be detected through liquid chromatography–mass spectrometry (LC–MS) based target analyses (5). However, target analyses do not seek to identify new or emerging contaminants; they solely focus on looking for what is known. For the "known unknowns," a suspect screening approach enables the detection of already described compounds that are present in chemical databases (6,7). Finally, screening for TPs means dealing with many millions of potential compounds, and for these "unknown unknowns," a reliable nontargeted screening (NTS) approach is essential. LC–HRMS is highly relevant here, enabling NTS that is fundamental to broader detection and accurate identification of TPs (8).

NTS identifies all measurable features (accurate mass-retention time pairs) within water samples (8). Features can be clustered based on feature intensity trend profiles from treatment processes, and can then be further categorized by risk. This approach facilitates the investigation of the identified clusters and their respective responses to relevant bioassays, making it possible to relate the chemistry to biological processes and fully assess the risks these compounds pose.

This study used LC–HRMS in combination with a novel data analysis workflow to screen water samples for OMPs and their TPs to examine the effectiveness of different water treatment methods, using bioassays to relate toxic effects to the detected compounds.

Overall Analytical Approach

The focus of this study was to detect and identify OMPs and their TPs at different stages of the water treatment processes using NTS. Figure 1 illustrates the overall NTS identification approach used, which involved moving from a confidence level of 5, representing all the features identified in a sample (based on mass, retention time, and intensity), to a confidence level of 1, where the unique structure of an individual TP is determined, and its identity confirmed (9). The process includes looking at molecular formula and structure, based on multiple different possible structures, the examination of spectral similarity, and final confirmation with a reference standard. Because NTS generates large numbers of features, prioritization criteria were applied to reduce the number requiring identification.

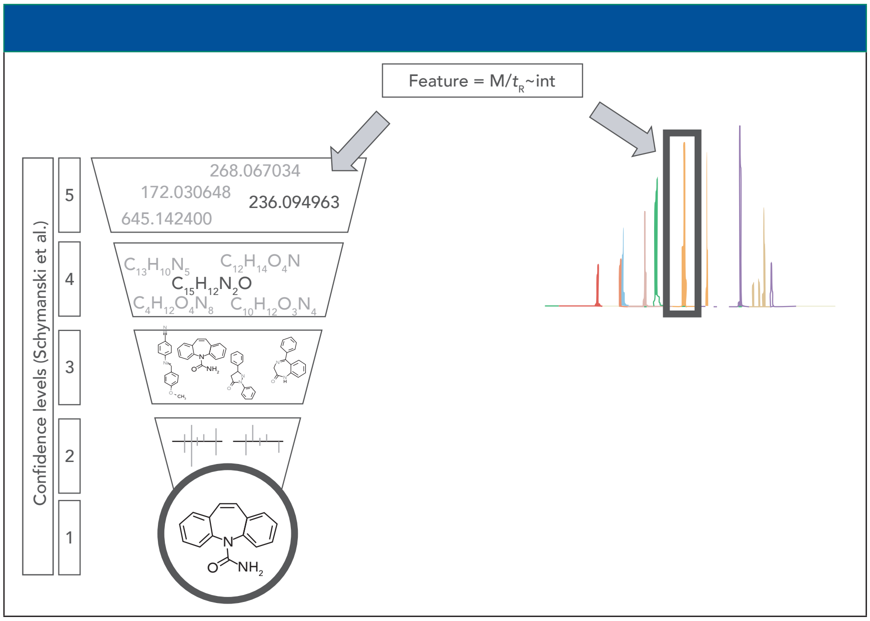

Figure 1: Non-targeted screening (NTS) identification approach.

Methodology

Spiking and Sampling

Three different drinking water treatment pilot installations were studied, each of which employed a different treatment protocol (Table I). To assess the effectiveness of each water treatment approach, 48 different OMPs, selected based on their presence in surface water, toxicity, available knowledge of treatment options, chemical properties, detectability, and availability, were spiked into the source water of each installation.

Pre- and post-treatment samples (with sampling after each treatment stage for installations 1 and 2) were analyzed using LC–HRMS. Targeted analysis and NTS workflows were applied to determine OMP removal rates, the presence of parent compounds, and formation of TPs.

Following preparation in flasks prerinsed with acetone and petroleum ether, and containing internal standards, each sample was filtered and split into three separate vials. From each vial, 100 µL of the sample was injected per LC–HRMS analysis. A range of predefined bioassays were used to examine compound toxicity, to help prioritize the identification of unknowns.

Table I: Water sources and treatment methods

Pilot Plant	Treatment Method	Source Water
1	Advanced oxidation using ozone (O_3)/hydrogen peroxide (H_2O_2) followed by ultraviolet (UV)/H_2O_2	Afgedamde Maas
2	UV/ H_2O_2 followed by granular activated carbon (GAC)	Ijsselmeer water
3	Ultrafiltration (UF) and reverse osmosis (RO)	Pre-treated Ijsselmeer water (drum sieves, coagulation/sedimentation, and rapid sand filters)

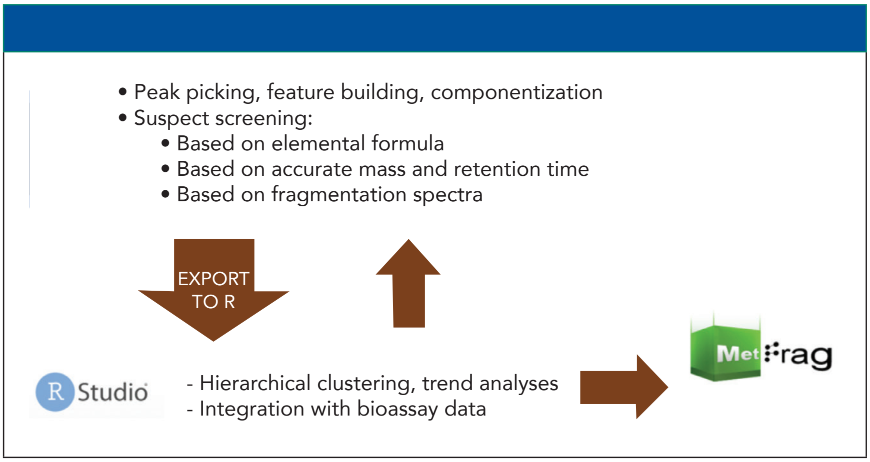

Figure 2: Non-targeted screening (NTS) data analysis workflow.

LC–HRMS Conditions

Chromatographic separations were performed on a Thermo Scientific Vanquish ultrahigh-pressure liquid chromatography (UHPLC) system, using an XBridge BEH C18 XP reversed-phase column (Waters Corporation) operating at 25 °C with an acetonitrile gradient.

Mass spectrometric data were collected on a Thermo Scientific Orbitrap Fusion Tribrid mass spectrometer, with a heated electrospray ionization source, using 120,000 FWHM resolution in full scan acquisition over the range of 50–1000 *m/z*. This was followed by data-dependent tandem mass spectrometry acquisition (DDA), selecting the top eight most intense peaks for fragmentation using stepped higher-energy collisional dissociation (HCD) energies of 20, 35, 50, and 15,000 FWHM resolution.

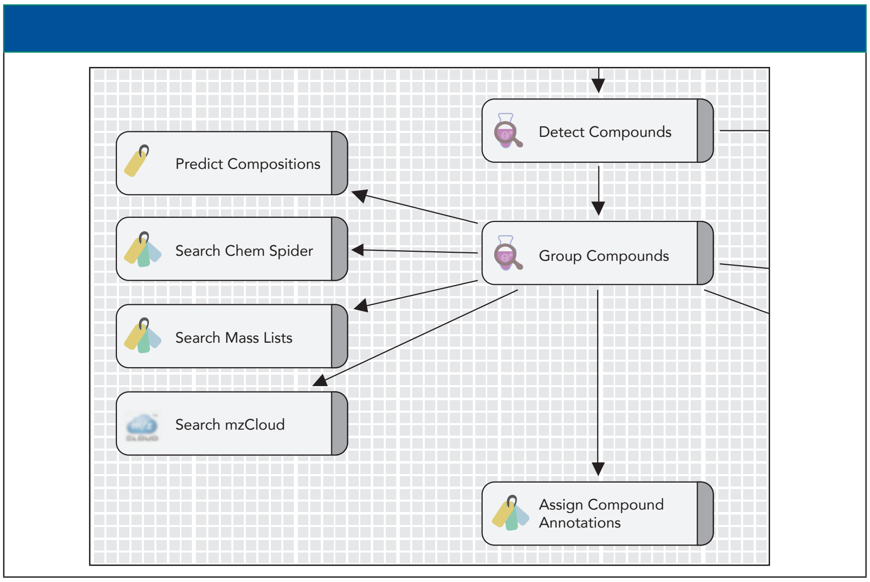

Figure 3: Software-enabled suspect screening using a variety of approaches.

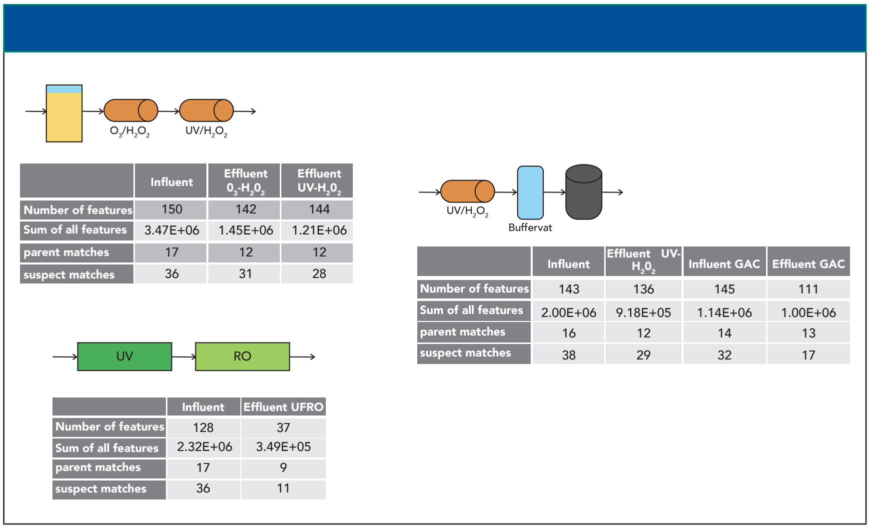

	Influent	Effluent 0_3-H_20_2	Effluent UV-H_20_2
Number of features	150	142	144
Sum of all features	3.47E+06	1.45E+06	1.21E+06
parent matches	17	12	12
suspect matches	36	31	28

	Influent	Effluent UFRO
Number of features	128	37
Sum of all features	2.32E+06	3.49E+05
parent matches	17	9
suspect matches	36	11

	Influent	Effluent UV-H_20_2	Influent GAC	Effluent GAC
Number of features	143	136	145	111
Sum of all features	2.00E+06	9.18E+05	1.14E+06	1.00E+06
parent matches	16	12	14	13
suspect matches	38	29	32	17

Figure 4: The results of assessing influent and effluent samples for feature count and suspect vs. parent.

Samples were measured in triplicate, with blank samples run every 5–10 samples to check for any carryover or contamination, as well as system performance through checking internal standards (IS).

Data Analysis

A mix of commercial software, open-source packages, and R-scripts were used for data analysis. The NTS data analysis workflow utilized Thermo Scientific Compound Discoverer software for peak picking, feature building, componentization, and identification of "knowns," "known unknowns," and elucidation of "unknown unknowns." Suspect screening was based on elemental formula, accurate mass and retention time, and fragmentation spectra via tandem mass spectrometry (MS/MS) data searching, using the Thermo Scientific mzCloud mass spectral fragment library and Thermo Scientific mzLogic data analysis algorithm to rank suspect candidates when there were no library matches. Data were then exported to the "R" programming language for hierarchical clustering, trend analyses, and integration with bioassay data (Figure 2).

Results and Discussion

LC–HRMS was used to assess different water treatments for their effects on TP formation and degradation. Data analysis enabled compound detection followed by suspect screening using a variety of approaches (Figure 3). These approaches included taking predicted compositions and searching molecular formulas in compound databases, and screening acquired spectra against spectral libraries of environmentally relevant compounds. Suspect screening was also conducted based on accurate mass, using the NORMAN SusDat database (10) of around 40,000 environmentally relevant compounds with their structures, which were imported into Compound Discoverer, as well as tailored lists of experimentally detected and predicted TP suspects.

For compounds that do not exist in any databases, the "unknown unknowns," there is a need to predict TPs, for which a range of tools were used based on rules for biotic and abiotic transformation processes (11,12) and metabolic logic (13). Fragmentation spectra were assessed against the experimental spectra in mzCloud with the application of mzLogic to rank order the suspect candidates retrieved from the multiple data sources used facilitating identification of compounds not in a spectral library.

Figure 4 shows the results of assessing influent and effluent samples for feature count and suspect versus parent (spiked in compounds) matches. Notably, advanced oxidation treatment resulted in 144 features in the final effluent, 28 of which were suspect matches and 12 were parent matches. Ultrafiltration, in combination with reverse osmosis, resulted in 37 features, of which 11 were suspect matches and 9 were parent matches. The overall high number of features across all three treatments meant that some form of prioritization would be required. Data also showed that degradation of the parent compounds and TP formation were water-source specific, that ultrafiltration reverse osmosis (UFRO) removed most compounds, and in cluster analysis, UFRO samples aligned with the experimental blanks (Figure 5).

Ahead of any prioritization, these data were processed with mzCloud, which allowed immediate identification of some OMPs, but many more were not present in the database. The first step in prioritizing the identification of the remaining features was to apply hierarchical clustering analysis to the data from all the samples. This enabled the detection of feature intensity trend profiles. Compounds clustered depending on whether they were removed or formed by a particular water treatment step.

The profiles for the advanced oxidation treatment steps O_3/H_2O_2, followed by UV/H_2O_2, are visualized in Figure 6. These show the influent for the process and effluent after O_3/H_2O_2, and again after UV/H_2O_2. Nine clusters emerged where the features either increased or decreased. Clusters 2, 4, 6, 7, and 9 showed an increase in features indicating these should be identified as a priority. An alternative approach to assessing the effectiveness of treatment is to look at the overall increase, reduction, or no change in features. The combined value in this treatment indicates that about 20% of features increase, and although this means identifying a fifth of features, it also represents a fivefold reduction in features through the treatment process.

Further prioritization can be achieved by including effect-based data. Here, NTS data were integrated with the results of bioassays, in this case, the standard Ames test for mu-

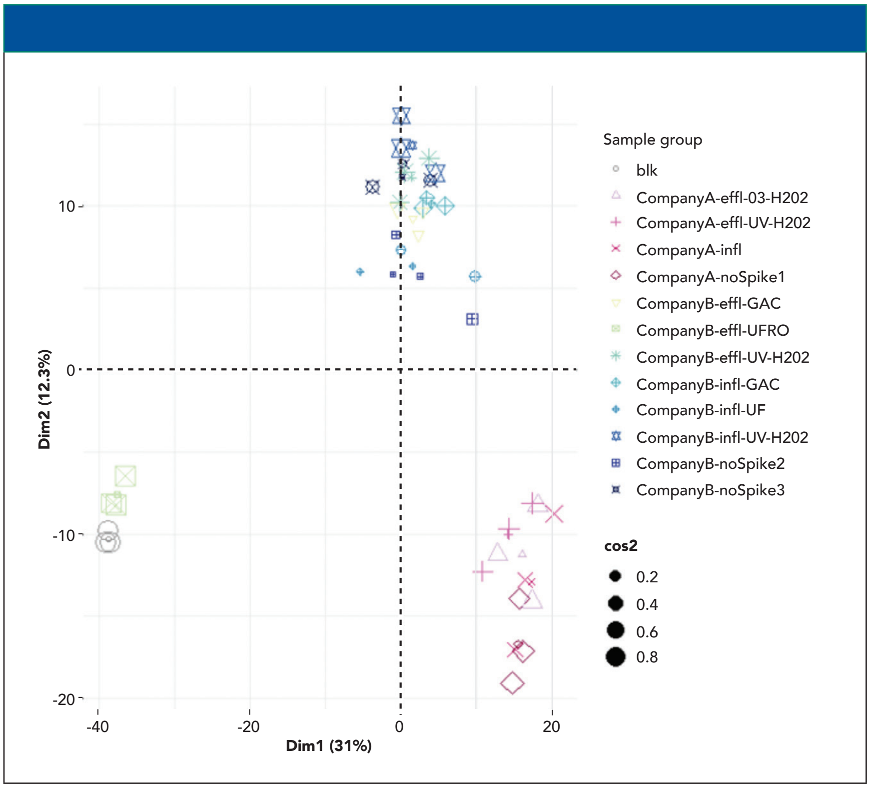

Figure 5: Degradation of the parent compounds and TP formation were water-source specific (15).

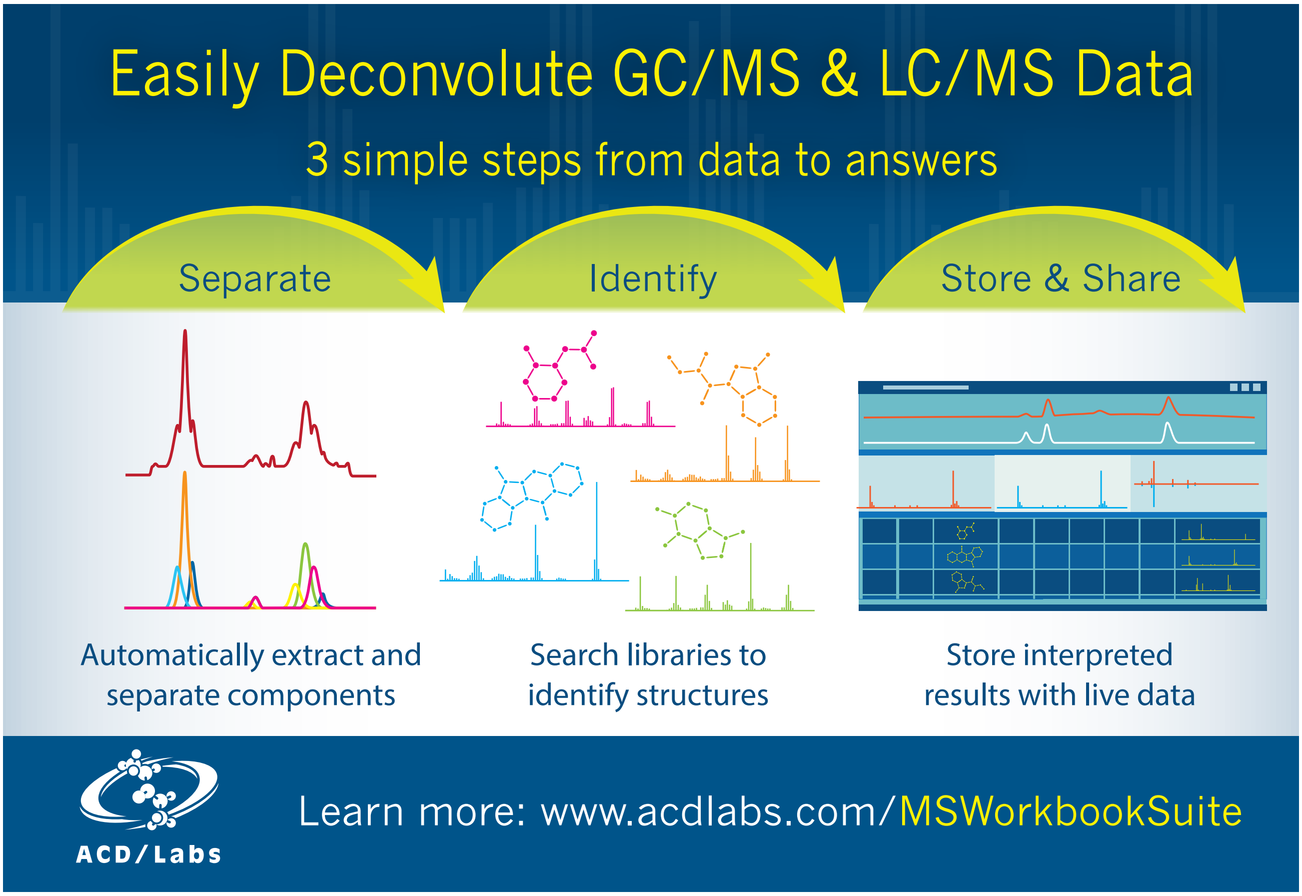

tagenicity and a range of chemical activated luciferase expression (CALUX) bioassays to identify toxic endpoints for substances, such as hormone disruption and anti-estrogenic receptors (14).

Integration of the data highlighted the presence of compounds that have potentially harmful effects, with correlation between the bioassay results and clusters 4, 7, and 9. The features occurring in clusters 4, 7, and 9 were therefore revisited in Compound Discoverer to try to identify them, with the associated data including peak shape, MS1 spectrum, isotopic pattern, and whether it provided a hit on the mass list (NORMAN SusDat). Suspect TP candidates were then ranked and identified based on spectral similarity. For one such TP with a molecular formula of $C_{24}H_{30}O_6$, the search results returned two possible compounds with differing mzLogic scores of 67 and 21 (Figure 7), providing insights as to the potential structural characteristics and putative structure for this unknown. Figure 8 indicates the acquired sample spectrum compared with the library spectrum for bis(4-ethybenzylidene)sorbitol, demonstrating that NTS can facilitate the confident identification of TPs, something that would not have been possible through other established means.

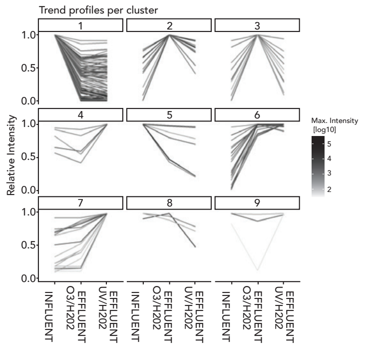

Non-target screening data	Decreasing intensity (% features)	Same intensity (% features)	Increasing intensity (% features)
$O3/H_2O_2$	61.8%	13.5%	24.7%
UV/H_2O_2	19.7%	66.9%	13.5%
Combined	61.8%	18.5%	19.7%

Figure 6: Trend profiles for the advanced oxidation treatment steps O_3/H_2O_2 followed by UV/H_2O_2 (15).

Conclusion

Increasing chemical use, and the discharge of industrial and personal waste into watercourses, are responsible for the growing presence of OMPs and their TPs in drinking water sources. This increase is driving the need to detect and remove these hazardous contaminants from water to ensure it is safe for human consumption. The large number of potential compounds, along with their extensive chemical diversity, poses significant challenges, and means targeted chemical analysis alone is no longer sufficient to determine drinking water quality and assessing the effects of treatment processes.

The data from this study demonstrate the utility of NTS in enabling a more complete analysis of samples, ensuring higher standards of water quality. Incorporating powerful NTS methods, using high-resolution accurate mass spectrometry into water quality assessment workflows, supports the development of an optimized, risk-based water monitoring strategy. This approach identifies features that potentially pose a risk to human health or the environment, and improves the identification of "unknown unknowns," allowing decisions to be made in relation to water treatment processes. It also provides the opportunity to monitor water treatment steps and

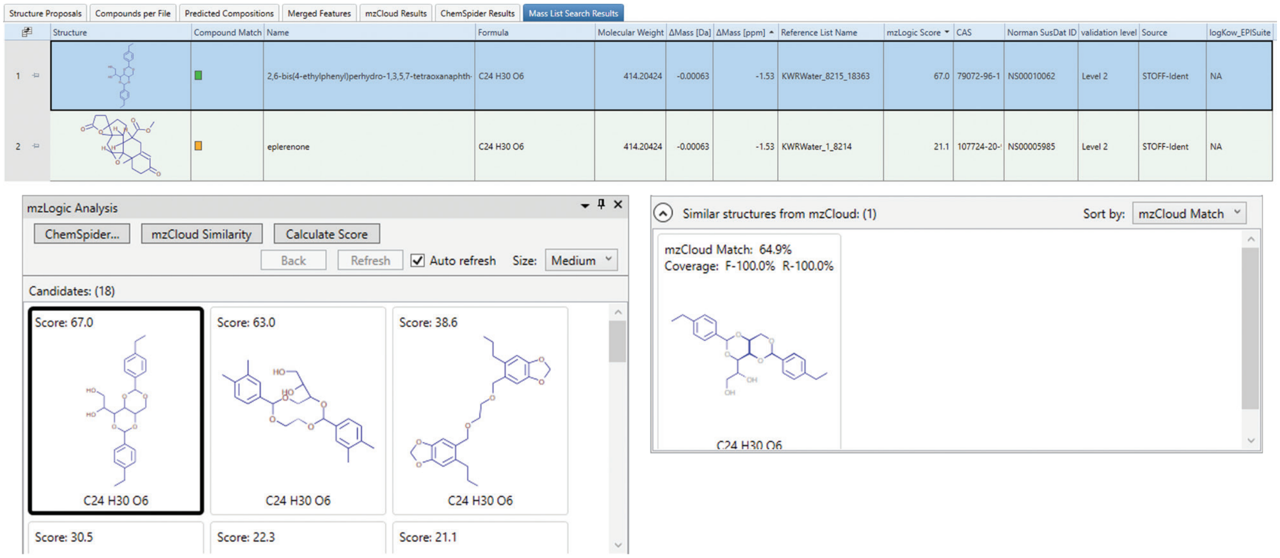

	Structure	Compound Match	Name	Formula	Molecular Weight	ΔMass [Da]	ΔMass [ppm]	Reference List Name	mzLogic Score	CAS	Norman SusDat ID	validation level	Source	logKow_EPISuite
1		🟩	2,6-bis(4-ethylphenyl)perhydro-1,3,5,7-tetraoxanaphth-	C24 H30 O6	414.20424	-0.00063	-1.53	KWRWater_8215_18363	67.0	79072-96-1	NS00010062	Level 2	STOFF-Ident	NA
2		🟧	eplerenone	C24 H30 O6	414.20424	-0.00063	-1.53	KWRWater_1_8214	21.1	107724-20-	NS00005985	Level 2	STOFF-Ident	NA

Candidates: (18)

Score: 67.0 C24 H30 O6

Score: 63.0 C24 H30 O6

Score: 38.6 C24 H30 O6

Score: 30.5

Score: 22.3

Score: 21.1

Similar structures from mzCloud: (1)

mzCloud Match: 64.9%
Coverage: F-100.0% R-100.0%
C24 H30 O6

Figure 7: For one potentially hazardous TP the mass list gave two different compounds.

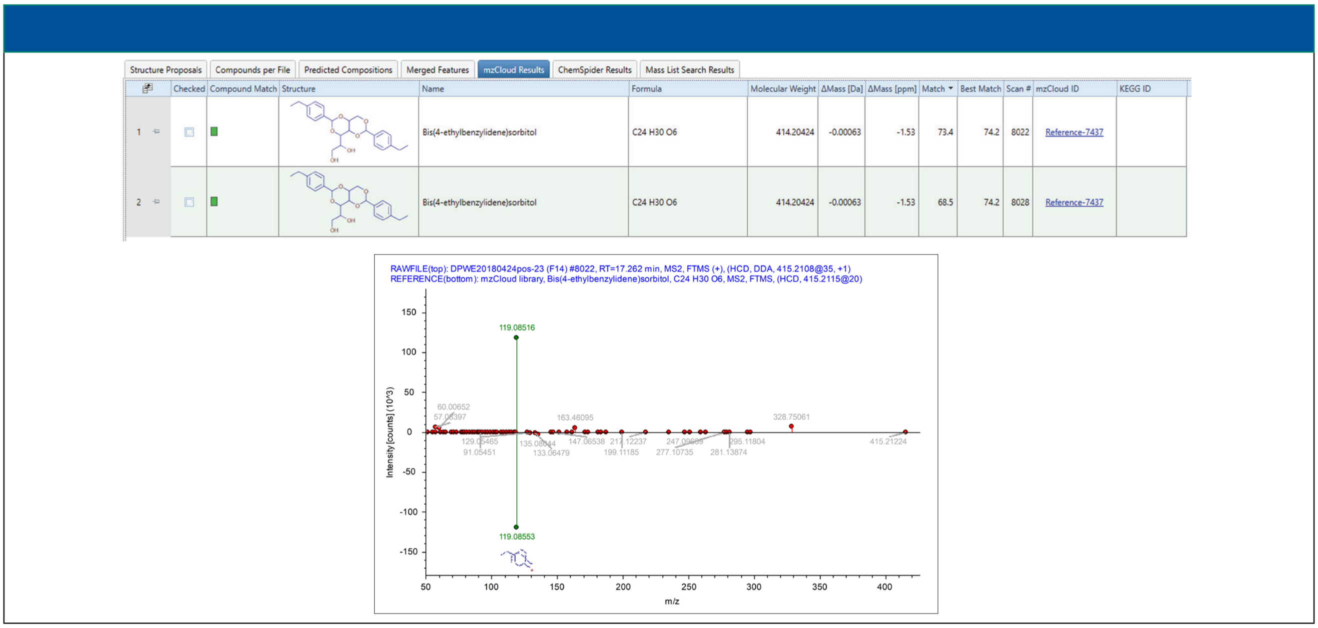

	Checked	Compound Match	Structure	Name	Formula	Molecular Weight	ΔMass [Da]	ΔMass [ppm]	Match	Best Match	Scan #	mzCloud ID	KEGG ID
1	☐	🟩		Bis(4-ethylbenzylidene)sorbitol	C24 H30 O6	414.20424	-0.00063	-1.53	73.4	74.2	8022	Reference-7437	
2	☐	🟩		Bis(4-ethylbenzylidene)sorbitol	C24 H30 O6	414.20424	-0.00063	-1.53	68.5	74.2	8028	Reference-7437	

RAWFILE(top): DPWE20180424pos-23 (F14) #8022, RT=17.262 min, MS2, FTMS (+), (HCD, DDA, 415.2108@35, +1)
REFERENCE(bottom): mzCloud library, Bis(4-ethylbenzylidene)sorbitol, C24 H30 O6, MS2, FTMS, (HCD, 415.2115@20)

Figure 8: The TP spectrum compared with the library spectrum for bis(4-ethybenzylidene) sorbitol.

improve drinking water monitoring for known and unknown contaminants to protect public health.

Consequently, NTS using high-resolution accurate mass spectrometry is becoming an essential tool for water quality monitoring due to the increased presence of emerging contaminants with water sources. With the ability to rapidly provide in-depth, high-quality MS^n data, and comprehensively triangulate multiple data sources and cheminformatics tools to determine contaminants and identify the compounds, HRAM MS will continue to facilitate the detection of established and emerging contaminants in water sources.

Acknowledgments

The author acknowledges Dennis Vughs, Annemieke Kolkman, Thomas ter Laak, Milou Dingemans, Cheryl Bertelkamp, Bas Wols, Danny Harmsen, Wolter Siegers (KWR), Bram J.Martijn (PWN), Wim A.Oorthuizen (Dunea), Camilla di Marcantonio (Sapienza University of Rome) and the Dutch drinking water utilities Dunea, PWN, Evides and Waternet for funding.

References

(1) Access Science Briefing, *Removing Organic Micropollutants from Wastewater.* Last reviewed 2016. https://www.accessscience.com/content/removing-organic-micropollutants-from-wastewater/BR0927161 (Accessed 9 December 2019)

(2) A.C. Belfroid, M. van Drunen, M.A. Beek, S.M. Schrap, C.A. van Gestel, and B. van Hattum, *Sci. Total Environ.* **222,** 167–183 (1998).

(3) C.J. Sinclair and A.B.A. Boxall, *Environ. Sci. Technol.* **37,** 4617–4625 (2003).

(4) C.M. de Jongh, P.J.F. Kooij, P. de Voogt, T.L. ter Laak, *Sci. Total Environ.* **427–428,** 70–77 (2012).

(5) W. Brack, J. Hollender, M.L. de Alda, C. Müller, T. Schulze, E. Schymanski, J. Slobodnik, and M. Krauss, *Environ. Sci. Eur.* **31,** 62 (2019).

(6) A.D. McEachran, J.R. Sobus, and A.J. Williams, *Anal. Bioanal. Chem.* **409,** 1729–1735 (2017).

(7) E.L. Schymanski, and A.J. Williams, *Chemicals Environmental Science & Technology* **51,** 5357–5359 (2017).

(8) J. Hollender, E.L. Schymanski, H.P. Singer, and P.L. Ferguson, *Environ. Sci. Tech.* **51**(20), 11505–11512 (2017) DOI: 10.1021/acs.est.7b02184.

(9) E.L. Schymanski, J. Jeon, R. Gulde, K. Fenner, M. Ruff, H.P. Singer, and J. Hollender, *Environ. Sci. Tech.* **48**(4), 2097–2098 (2014).

(10) Network of reference laboratories, research centres and related organisations for monitoring of emerging environmental substances. NORMAN Suspect List Exchange. https://www.norman-network.com/?q=suspect-list-exchange (Accessed 9 December 2019).

(11) K. Fenner, J. Gao, S. Kramer, L. Ellis, and L. Wackett, *Bioinformatics* **24,** 2079–2085 (2008).

(12) L. Blum, L.C. Schmid, E. Fenner, and K. von Gunten, *Environ Sci Process Impacts* **19,** 465–476 (2017).

(13) J. Schollee, *Linking Influent and Effluent Peaks from Biological Wastewater Treatment to Detect Relevant Nontarget Compounds*, SETAC Europe, Barcelona, Spain (2015), p. 2.

(14) M.B. Heringa, D.J.H. Harmsen, E.F. Beerendonk, A.A. Reus, C.A.M. Krul, D.H. Metz, and G.F. Ijpelaar, *Water Research* **45,** 366-374 (2011).

(15) A.M. Brunner, C. Bertelkamp, M.M.L. Dingemans, A. Kolkman, B. Wols, D. Harmsen, W. Siegers, B.J. Martijn, W.A. Oorthuizen, and T.L. ter Laak, *Sci. Total Environ.* **705**(135779), (2019), DOI: 10.1016/j.scitotenv.2019.135779.

Andrea Mizzi Brunner is the deputy team leader of the Chemical Water Quality and Health team at KWR Water Research Institute, in Nieuwegein, in the Netherlands. Direct correspondence to: andrea.brunner@kwrwater.nl

Optimized Explosives Analysis Using Portable Gas Chromatography–Mass Spectrometry for Battlefield Forensics

Advancements in technology enable deployment of field-friendly gas chromatography–mass spectrometry (GC–MS), so the value of the technique can be realized at the sample site. A primary benefit of deployment to the scene is the ability to analyze trace levels of threats, providing real-time information to support scene safety and other intelligence, so mission-critical decisions using confirmed information may be made. This capability is especially useful in situations where a sample degrades, changes, or is unstable during storage or transport, or when access to a laboratory is not an option. When explosives are encountered on the battlefield, GC–MS may be useful. In this research, a variety of commercial, military, and homemade explosives were analyzed using portable ion-trap GC–MS. Data from both ion-trap and quadrupole mass-spectral libraries were compared to establish whether portable ion-trap GC–MS is useful for the identification of explosives. Ion-trap mass spectral data can be different from quadrupole data due to ion chemistry and other ion interactions, including space charge that may occur during ion trapping. These results show that, although mass spectral data are sometimes different from quadrupole mass spectral data, portable ion-trap GC–MS is useful for performing confirmatory identification of explosives in the field. The forensic value of this capability is also considered.

Kayla Moquin, Alan G. Higgins, Pauline E. Leary, and Brooke W. Kammrath

Portable gas chromatography–mass spectrometry (GC–MS) instrumentation has enabled the confirmatory analysis of explosive residues in the field. For battlefield forensics, portable GC–MS instruments are used for the detection and confirmatory identification of pre- and post-detonation threats. In addition, these systems provide information regarding the source of explosives based on the detection and identification of trace-level chemicals in the sample. The use of portable GC–MS is valuable for supporting scene safety, gathering intelligence, and providing investigative and adjudicative information about explosives events.

It is important to recognize that GC–MS in the laboratory has historically been used for some of these same purposes, but there are significant benefits to performing the analysis at the scene. First, on-scene analysis enables the development of render-safe procedures based upon real-time threat identification and assessment. Second, intelligence turnaround time to support offensive operations is significantly improved. Commanders are empowered to make actionable decisions using reliable, confirmed information. Third, GC–MS results in real time can help guide and optimize scene processing. Finally, analysis at the sample site enables the most accurate evaluation of the scene. Results are representative of the scene at the time of analysis, not at some later date when samples are received and analyzed at the laboratory. This timeliness is especially relevant for this type of physical evidence, because, aside from the danger associated with storage and transport of explosive evidence, some explosives have relatively high vapor pressures, and will evaporate or sublimate during transport to the laboratory.

Portable GC–MS systems were initially introduced to the market almost 25 years ago. Since this time, the design and performance of these systems has evolved (1,2), and there are currently a number of portable GC–MS options available to both scientists and non-scientists performing field analysis. These systems include both quadrupole and ion-trap designs. Quadrupole systems offer the benefit of generating classical mass spectra that are more easily interpreted and directly comparable with spectra in the National Institute of Standards and Technology (NIST) MS database. Ion-trap systems are desirable for field use, because they can run at higher operating pressures. The pumps required to achieve and maintain these higher pressures are more field friendly than the chemical pumps that were historically needed to achieve and maintain the operating pressures required of portable quadrupole systems. However, spectra generated using ion-trap systems may exhibit ion-chemistry events such as dimer formations occurring in the trap (2), and, therefore, are not always directly comparable with mass spectra within the NIST MS database. In addition, space charge is sometimes observed. Space charge occurs when the force of ion-ion repulsions inside the trap become too great, and can result in incorrect *m/z* assignments. Space charge further complicates spectral library matching. Library search results are frequently critical to end users of portable GC–MS systems who rely on library matching to achieve successful results in the field.

To evaluate the potential use of portable ion-trap GC–MS analysis for the on-scene evaluation of explosive evidence, explosive standards were analyzed and compared with the proprietary library of the system and with the NIST MS database spectra to establish effectiveness of search results for these explosive standards. In addition, explosives samples received from international law-enforcement organizations were analyzed using portable ion-trap GC–MS, and results generated were reviewed to evaluate capabilities of the technology for analyzing the explosive-related components in these recovered samples.

Table I: Law-enforcement explosive evidence samples

Sample Number	Explosive Type	Sample Description
1	C4	C4 tagged with 0.1% DMNB
2	C4	C4 tagged with MNT
3	C4	C4
4	Detasheet	Detasheet (1)
5	Detasheet	Detasheet (2)
6	Dynamite	Dynamite (1)
7	Dynamite	Dynamite (2)
8	Dynamite	Dynamite (3)
9	Dynamite	Dynamite (4)
10	Pentex	Pentex (1)
11	Semtex	Semtex (1)
12	Semtex	Semtex tagged with 0.1% MNT
13	Semtex	Semtex tagged with Taggant
14	Semtex	Semtex H (1)
15	Semtex	Semtex H tagged with MNT
16	Semtex	Semtex H (2)
17	Semtex	Semtex (2)
18	Tetryl	Tetryl
19	TNT	TNT (1)
20	TNT	TNT (2)

Table II: Results of detection of explosive standards using portable ion-trap GC–MS

Explosive	Detection of Target in Explosive Standard
DMNB	Reliably detected
DNT	Reliably detected
EGDN	Reliably detected
HMTD	Not detected
PETN	Reliably detected
RDX	Not detected
TATP	Reliably detected
TNB	Reliably detected
TNT	Reliably detected

Table III: Library-searching results from explosive standard samples

Explosive	Identification Against Proprietary Ion-Trap Library on the Portable System	Identification Against NIST Mass MS Database
DMNB	Excellent	Excellent
DNT	Excellent	Excellent
EGDN	Excellent	Excellent
PETN	Excellent	Excellent
TATP	Excellent	~50/50
TNB	Not in library	Excellent
TNT	Excellent	Excellent

Materials and Methods

Materials

The portable GC–MS system used in this research directly links a low thermal mass resistively heated capillary column with a miniaturized toroidal ion-trap mass spec-

Table IV: Explosives included in the proprietary library of the portable ion-trap GC–MS instrument

1,3-diethyl-1,3-diphenylurea (ethyl centralite)
2, 4-DNT
2,3-DNT
2,4-DNT
2,6-DNT
2-amino-4,6-dinitrotoluene (2-ADNT)
2-methyl-4-nitrotoluene
2-nitrotoluene (o-MNT)
3,4-DNT
3-nitrotoluene (m-MNT)
4-amino-2,6-dinitrotoluene (4-ADNT)
acetylacetone
ammonium acetate
benzoic acid
decane
dinitroglycerin
diphenylamine
DMNB
EGDN
hexane
HMTD
nitroglycerin
octane
pentane
PETN
RDX
sulfur (black powder)
TATP
tetryl
TNB
TNT

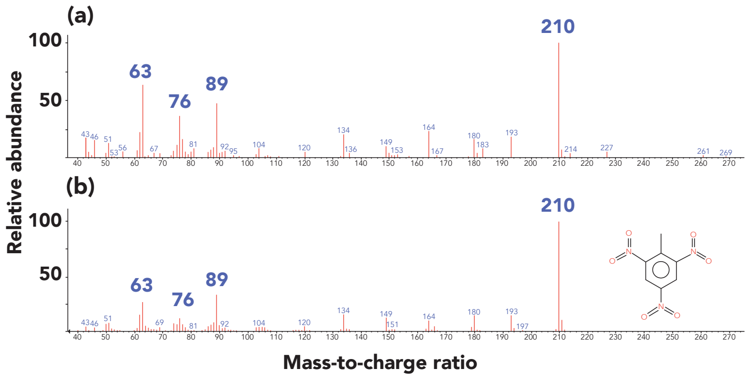

Figure 1: (a) Mass spectra of TNT from portable ion-trap GC–MS, and (b) the NIST MS database.

trometer (3–5). The GC column enables fast separation and thermal recovery (3-min analysis time) resulting in high throughput (approximately 5 min between injections). High throughput is always a desirable feature of analysis, but especially for field applications where scene-processing time may be limited or the scene itself may be dangerous. The toroidal ion-trap design is intended to increase trapping volume and, therefore, to minimize ion-ion repulsions. Regardless, the impact of both space charge and ion chemistry on the mass spectra generated may still be observed when using this system.

Equipment

The following equipment was used in this research:

- Smiths Detection Guardion portable GC–MS system with a GC capillary column; 5 m-long, Restek Corporation MXT-5 resistively heated, crossbond diphenyl-dimethylpolysiloxane, inner diameter 0.1 mm, film thickness 0.4 μm
- Leland Limited Incorporated disposable helium cartridge, 95 cc x 5/8 in helium filled, 2.4 g at 2500 psi
- Torion Technologies Custodian solid-phase microextraction (SPME) holder
- Supelco 23-gauge, 65-μm polydimethylsiloxane/divinylbenzene (PDMS/DVB) SPME fiber assembly
- Smiths Detection Guardion performance validation mixture sample
- Microsyringe
- Headspace GC–MS vials.

Explosive standards were purchased from AccuStandard, Inc., in New Haven, Connecticut, and include:

- 2,3-dimethyl-2,3-dinitrobutane (DMNB), 100 μg/mL in acetonitrile, CAS#3964-18-9
- 2,4-dinitrotoluene (2,4-DNT), 1000 μg/mL in methanol, CAS#121-14-2
- ethylene glycol, dinitrate (EGDN), 100 μg/mL in acetonitrile:methanol (95:5), CAS#628-96-6
- hexamethylene triperoxide diamine (HMTD), 100 μg/mL in acetonitrile, CAS#283-66-9
- pentaerythritol tetranitrate (PETN), 1000 μg/mL in methanol, CAS#78-11-5
- 1,3,5-trinitro-1,3,5-triazinane (RDX), 1000 μg/mL in methanol:acetonitrile (50:50), CAS#121-82-4

- triacetone triperoxide (TATP), 0.1 mg/mL in acetonitrile, CAS#17088-37-8
- 1,3,5-trinitrobenzene (TNB), 1000 μg/mL in methanol:acetonitrile (50:50), CAS# 99-35-4
- 2,4,6-trinitrotoluene (TNT), 1000 μg/mL in methanol:acetonitrile (50:50), CAS#118-96-7.

Law-enforcement explosive evidence samples were received from various international law-enforcement organizations. These samples are detailed in Table I. The 20 samples are each from a different origin. The explosive type, as well as the sample description for each, was provided by the contributing organization. Aside from the details shown in Table I, no further information about the history of these samples was provided to the authors.

Methods

Sampling

Prior to all sampling, the SPME fiber was verified to be clean by performing an analysis using the GC–MS method described below. If chemicals were detected, the SPME fiber was continually cleaned by heating, until no chemicals were detected on the fiber. Explosive standard solutions were sampled using the direct-deposition method. Law-enforcement explosive samples were analyzed using either SPME headspace sampling, direct deposition, or both methods.

SPME Headspace Sampling

Between 100 and 500 mg of sample was transferred to a GC–MS headspace vial. The vial was closed and then stored at 22 °C for at least 2 h. The headspace was then sampled by piercing the vial cap with the needle end of the SPME holder containing the SPME fiber and exposing the fiber for a specified period of time. Sampling times were variable and ranged from 10 min to 40 min.

Direct Deposition

For explosive standards, explosive amounts between 20 and 200 ng were directly deposited using a microsyringe onto the coated portion of the SPME fiber, and allowed to dry for up to 5 min to allow evaporation of the solvent. Although attempts were made to control the amount of sample deposited onto the fiber, no attempts to provide quantitative analysis of these data were made. For law-enforcement samples, between 100 and 500 mg of sample was dissolved in 10 mL of acetone and stored at 22 °C for at least 2 h. Then, 10 μL of the sample solution was directly deposited using a microsyringe onto the coated portion of the SPME fiber, and allowed to air dry for up to 5 min, to allow evaporation of the solvent.

GC–MS Analysis

Performance of the system was tested at the start of every work day. Performance testing evaluates GC, MS, and library search performance. To perform this testing, a standard containing 13 chemicals is analyzed. These 13 chemicals have expected retention-time values between 0 and 90 s. GC performance acceptance criteria requires that the retention times for all 13 chemicals must be the stated value ±2 s. MS performance includes tests for spectral quality, mass calibration, mass resolution, ion statistics, space charge, signal-to-noise ratio, and sensitivity. Library- search testing verifies the system is matching substances as expected against the system's proprietary library. The system always passed all performance-test criteria prior to use.

Table V: Automatic library-search results for the explosives-related identifications in law-enforcement samples

Sample Number	Sample Description	Explosives Detected (Headspace Sampling)	Explosives Detected (Direct Deposition)	False Automatic Detection and Identification
1	C4 tagged with 0.1% DMNB	DMNB	not tested	EGDN
2	C4 tagged with MNT	no explosive detected	no explosive detected	EGDN
3	C4	not tested	no explosive detected	
4	Detasheet (1)	EGDN	PETN, EGDN	
5	Detasheet (2)	EGDN	not tested	
6	Dynamite (1)	EGDN, dinitroglycerin	EGDN	
7	Dynamite (2)	EGDN, dinitroglycerin	EGDN	
8	Dynamite (3)	EGDN, 2,3-DNT, dinitroglycerin	EGDN, 2,3-DNT, 3,4-DNT	
9	Dynamite (4)	not tested	EGDN, NG	PETN
10	Pentex (1)	no explosive detected	PETN, TNT	
11	Semtex (1)	not tested	PETN	dinitroglycerin
12	Semtex tagged with 0.1% MNT	not tested	MNT, PETN	dinitroglycerin
13	Semtex tagged with Taggant	not tested	PETN	dinitroglycerin
14	Semtex H (1)	not tested	PETN	EGDN and dinitroglycerin
15	Semtex H tagged with MNT	not tested	PETN, MNT	
16	Semtex H (2)	not tested	PETN	
17	Semtex (2)	not tested	PETN	dinitroglycerin
18	tetryl	none detected	None automatically identified; required manual review of data	
19	TNT (1)	2,3-DNT, 2,4-DNT	TNT	RDX
20	TNT (2)	not tested	TNT	RDX

The performance-test procedure used was the procedure recommended by the instrument manufacturer.

The system used in this research is deployed with a single GC–MS method. This method is linked to a proprietary library, as well as a condensed version of the NIST MS database. It is required that, if the user wants to search these libraries at the time of analysis, the deployed GC–MS method must be used. Although there is some deviation from that method that is tolerated, the use of some GC settings, including ramp rate, begin temperature, and begin hold time are required. This is because library search criteria use retention times when searching the proprietary library, and retention index when searching the condensed NIST MS database. It is possible to change these settings, but this would require either library development (if automatic library searches were required), or manual interpretations of GC–MS results.

The method's standard GC settings (which were used for this research) are as follows:

- Injector temp.: 270° C
- Transfer line temp.: 270° C
- Ramp rate: 2 °C/s
- Begin temp.: 50 °C
- Begin hold time: 10 s
- End temp.: 296 °C
- End hold time: 47 s
- Split: Off
- Sample desorption time: 10 s

Results

Explosive Standards

A manual review of all data from the explosive standard samples was performed, and chromatographic peaks and characteristic mass spectra for seven of the nine samples were reliably detected. For these seven samples, detections were possible at both low and high concentrations, and at all inlet temperatures. For two of the nine standards, no chromatographic peak for the explosive was detected. In addition, expected target ions were actively searched in the region of their expected retention and across the entire chromatogram in each data file to confirm the negative findings of the chromatographic data review. Table II summarizes the detection results from the manual review of the GC–MS data from the explosive standards.

RDX was not detected in the standard sample. As is described later, it also was not detected in any law-enforcement samples expected to contain RDX. Although no RDX was detected, it is assumed that the system in its current configuration is capable of detecting RDX because this substance is programmed into the proprietary library for the system. This library is purported to contain library data generated using the system with its deployed method. The library entry describes GC retention values and MS fragments consistent with those reported in the NIST MS database for RDX, so it is assumed the system is capable of detecting RDX, not just its degradation products, impurities, or other contaminants. The failure to detect this compound using the portable GC–MS may be due the inlet temperature or transfer line temperatures being too high. As has been reported by other researchers, the thermally sensitive nature of some explosives can cause them to degrade when introduced to the high temperatures of the inlet (6). To address this potential expectation, the systems inlet temperature was lowered to 210 °C, but no RDX was detected. It is likely that a method for this substance at even lower temperature would be required for its detection.

HMTD was also not detected in the standard sample under any analysis conditions. It was also not detected in any of the law-enforcement samples, although none of the law-enforcement samples were expected to contain this explosive. In accordance with the NIST MS database, HMTD has an estimated non-polar retention index value of 1619, and its three most intense mass fragments at *m/z* values in descending order of intensity of 208, 88, and 45. As such, this explosive would be expected to exhibit a retention time in this portable GC–MS under these analysis conditions of approximately 101.5 s. No chromatographic peaks were observed at or around this retention time. It is also important to note that the entry for this explosive in the proprietary library of the portable GC–MS system listed the anticipated retention time of 34.4 s for HMTD (RI value of approximately 770), with its most intense mass fragments in descending order of intensity of 73, 74, and 44. The significant discrepancy between the retention values reported in the NIST MS database and the proprietary library entry of the portable GC–MS system indicate the entry in the proprietary library is not representative of HMTD, and is potentially a degradation product, impurity, or other contaminant.

In addition to performing a manual review of the data, all GC–MS data files for the seven detected explosives were searched against the library of the portable GC–MS system. This search uses its own proprietary search algorithm. Of the seven samples detected, only six were in the library. For the six explosives in the library, an automatic identification of the explosive sample was reliably made. The automatic identification occurred at both low and high concentrations, and at all inlet temperatures.

A search of each GC–MS data file for the seven detected explosives was also performed by comparing the mass spectrum at the chromatographic peak maximum of the explosive against the NIST MS database using the NIST MS database search software. For six of the seven samples, the highest probability hit always correctly identified the explosive substance. However, TATP was only identified as the top hit about 50% of the time. The ability to correctly identify TATP as the top hit against the NIST MS database was not attributable to sample load. It is important to note that searches against the NIST MS database only consider mass spectral data when generating a hit list. A summary of library searching results is shown in Table III.

Finally, the mass-spectral data from the ion-trap system were manually compared with NIST MS database quadrupole spec-

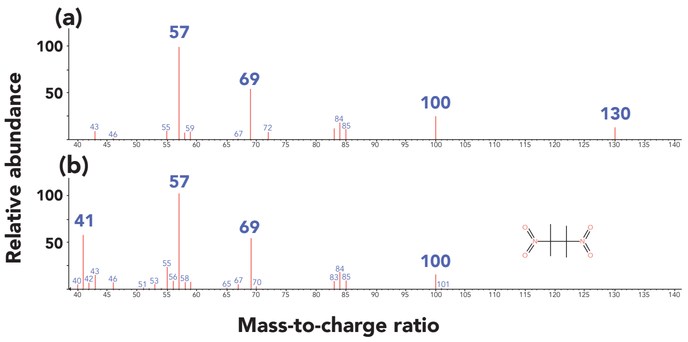

Figure 2: (a) Mass spectra of DMNB from portable ion-trap GC-MS, and (b) the NIST MS database.

Decreasing vapor pressure

nitromethane (NM)
hydrogen peroxide (HP)
diacetone diperoxide (DADP)
ethylene glycol dinitrate (EGDN)
triacetone triperoxide (TATP)
p-mononitrotoluene (p-MNT)
2,3-dimethyl-2,3-dinitrobutane (DMNB)
2,6-dinitroluene (2,6-DNT)
nitroglycerin (NG)
2,4-dintrotoluene (2,4-DNT)
1,3,5-trinitrobenzene (TNB)
ammonium nitrate (AN)
2,4,6-trinitrotoluene (TNT)
2,4,6-trinitromesitylene (TNM)
2,4,6-trinitro-m-cresol (TNC)
2,4,6-trinitrophenol (picric acid)
urea nitrate (UN)
2,4,6-trinitroaniline (TNA)
pentaerythritol tetranitrate (PETN)
N-methyl-N-(2,4,5-trinitrophenyl) nitramide (tetryl)
cyclotrimethylene trinitramine (RDX)
1,3-diamino-2,4,6-trinitrobenzene (DATB)
ammonium perchlorate (AP)
nitroguanidine
cyclotetramethylene tetranitramine (HMX)
1,3,5-triamino-2,4,6-trinitrobenzene (TATB)
hexanitrosilbene (HNS)
guanidine nitrate (GN)

Figure 3: Vapor-pressure values in order of decreasing vapor pressure.

tra. In most cases, as is evidenced in the automatic library search results, no significant differences were observed between the two types of spectra. Figure 1 shows the mass spectrum from the portable ion-trap system, along with the NIST MS database spectrum of TNT. Although small differences in peak intensities were observed across the spectrum, these spectra are generally consistent with each other. The most significant difference between the ion-trap and quadrupole spectra were observed in the spectra of DMNB. The ion-trap spectrum of DMNB had an additional ion fragment at *m/z* 130 that was not observed in the NIST MS database spectrum. This fragment had an intensity of about 13% of the most intense fragment in the spectrum (*m/z* 57). In addition, the ion fragment at *m/z* 41 was not observed in the ion-trap data. However, the ion-trap system is only specified to detect fragments of *m/z* 43 to 500. Therefore, not too much should be interpreted from its absence in this data. The ion-trap spectrum of DMNB from the portable ion-trap system and the NIST MS database spectrum of DMNB are shown in Figure 2.

The TATP data was also reviewed to investigate the cause of the missed identifications when searched against the NIST MS database. It is likely that the missed identifications are due to the simplicity of the mass spectrum of this explosive. The most intense fragment in the NIST MS database spectrum is *m/z* 43, followed by fragments at 58, 59, and 70, which have relative intensities to 43 of 13%, 11%, and 10%, respectively. There are spectra of many chemicals within the NIST MS database that have very similar spectra to TATP. The incorrect identifications of TATP when searched against the NIST MS database were all from chemicals that had very similar spectra to TATP. It was possible to sometimes, but not always, exclude the missed identifications due to inconsistencies between the retention time observed in the chromatogram from the ion-trap GC–MS system and the retention index reported in the NIST MS database.

Law-Enforcement Explosive Evidence Samples

Table IV details the explosive-related compounds included in the proprietary library of the portable ion-trap GC–MS system; Table V details the automatic library search results for the explosives-related identifications from the 20 law-enforcement samples. A manual review of all data was also performed. As previously mentioned, the system did not detect RDX. This is important because a number of samples contain RDX, including Semtex and C4. In addition, the system failed to automatically identify tetryl, even though tetryl was in the library. This is because this sample was slightly overloaded, and does not chromatograph well on this column. The poor chromatography coupled with column overload caused a shift in the observed retention time. This observed retention time was outside of the retention-time window of the library entry. Therefore, the substance was not identified.

Aside from missing RDX and tetryl, the system returned a few false automatic identifications including for EGDN in two of the three samples of C4 and one of the six samples of Semtex, PETN in one of the three dynamite samples, dinitroglycerin in four of the six samples of Semtex, and RDX in both TNT samples. Identifications were considered false if no chromatographic peak was present, but the software identified the substance. Such a result may occur when spectra are noisy and the chemical for identification has few or common mass fragments. For instance, the proprietary ion-trap library entry for dinitroglycerin contains only three fragments with *m/z* values of 46, 76, and 64, at 100%, 8%, and 1% intensities, respectively. It is reasonable to expect that these three fragments will be present in noisy data.

A review of the results also shows that there is value to analyzing explosive samples using both headspace and direct-deposition sampling. For instance, dinitroglycerin in dynamite samples was always observed in the headspace samplings, but never in the direct-deposition sampling. For TNT, DNT degradation products were observed in the headspace sampling, but not in the direct-deposition sampling. The reverse was true for the TNT that was not observed in the headspace sampling, but was reliably observed in the direct-disposition samples. The different results that occur from using the two sampling methods are not contradictory to each other; they enable a more complete assessment of the sample. Headspace sampling prior to sample dilution is useful for identifying the components of the sample with higher vapor pressures. Vapor-pressure values of explosives reported in the literature, for a number of reasons, are variable and sometimes contradictory (7–9), but Figure 3 summarizes the ranking order of vapor-pressure values of many explosives at 25 ˚C, calculated by Ewing and associates after an extensive review of values reported in the literature. (8)

Some final observations about these data are outside the initial scope of this research, but it is clear there is a significant amount of forensic value to this type of evidence. The ability to identify trace-level markers, such as taggants like DMNB and MNT, can be used to establish sample source. Further, it was possible to distinguish the two Detasheet samples. The plasticizers and other sample components generated chromatographic patterns that were easily distinguished. A more complete review of the chemical composition, including non-explosive components of each sample, may provide valuable investigative information.

Conclusion

Portable ion-trap GC–MS is a valuable tool for the evaluation of explosive evidence at the scene. Explosive standards for DMNB, DNT, EGDN, PETN, TATP, TNB, and TNT were reliably detected and identified using the automatic library search function of a portable GC–MS system when analyzed using the general test method deployed on the system. All explosives except TATP were also reliably identified when searched against the NIST MS database of quadrupole spectra. TATP was only identified 50% of the time when compared against the NIST MS database. It was not possible to either detect or identify RDX or HMTD using the general test method of the system.

In addition, 20 law-enforcement explosive evidence samples were analyzed, and explosives including 2,3-DNT, 3,4-DNT, dinitroglycerin, DMNB, EGDN, nitroglycerin, PETN, nitroglycerin, TNT, and MNT were automatically detected and identified by the system. These identification results were consistent with expectations of each sample's explosive composition. The inability of the method to detect RDX was significant, because both C4 and Semtex contain this explosive. Although not important for these samples (because none were expected to contain HMTD), the inability of the method to detect HMTD is significant, because this explosive is relatively easy to synthesize from starting materials that are readily available. It is possible that detection and identification of HMTD and RDX may be achieved by reduction of inlet and transfer line temperatures. It is also important to note that both the SPME headspace and direct-deposition sampling methods were valuable, and the results achieved using both methods frequently provided complementary information about the chemical composition of the sample.

Finally, automatic library identifications sometimes generated false-positive results. For this reason, it is important to manually review all automatic identifications. In all instances when the GC-MS data for a false-positive result was manually reviewed, it was evident from the data that the result was a false identification.

Acknowledgments

The authors would like to thank the international law-enforcement organizations for generously supplying explosive samples for this research. In particular, we are grateful for the support provided by the Connecticut State Police K9 Unit, and specifically TFC Jon Naples and TFC Brian Faughnan.

(1) C. Crume, History of Inficon HAPSITE: Maintenance Management, Support, and Repair. KD Analytical, http://www.kdanalytical.com/instruments/inficon-hapiste-history.aspx, (2009).

(2) P.E. Leary, B.A. Kammrath, and J.A. Reffner, *Enc. Anal. Chem.* **1–23** (2018). DOI: 10.1002/9780470027318.a9583.

(3) S.A. Lammert, A.A. Rockwood, M. Wang, M.L. Lee, E.D. Lee, S.E. Tolley, J.R. Oliphant, J.L. Jones and R.W. Waite, *J. Amer. Soc. Mass Spectrom.* **17,** 916–922 (2006). DOI: 10.1016/j.jasms.2006.02.009.

(4) P.E. Leary, G.S. Dobson, and John A. Reffner, *Appl. Spectrosc.* **70,** 888–896 (2016). DOI: 10.1177/0003702816638294.

(5) S.A. Lammert, W.R. Plass, C.V. Thompson and M.B. Wise, *Int. J. Mass Spectrom.* **212,** 25–40 (2001). DOI: 10.1016/S1387-3806(01)00507-3.

(6) J.R. Ash, Master of Science Thesis, Purdue University, Indianapolis (2016).

(7) H. Östmark, S. Wallin, and H.G. Ang, *Propell. Explos. Pyrot.* **37,** 12–23 (2012) DOI: 10.1002/prep.201100083.

(8) R.G. Ewing, M.J. Waltman, D.A. Atkinson, J.W. Grate, and P.J. Hotchkiss. *Trends Anal. Chem,* **42,** 35–48 (2013). DOI: 10.1016/j.trac.2012.09.010.

(9) M.J. Aernecke, T. Mendum, G. Geurtsen, A. Ostrinskaya and R.R. Kunz, *J. Phys. Chem. A* **119,** 11514–11522 (2015). DOI: 10.1021/acs.jpca.5b08929.

Kayla Moquin is a student researcher at the University of New Haven, in New Haven, Connecticut. **Alan G. Higgins** is an EOD Program Manager at Federal Resources, in Stevensville, Maryland. **Pauline E. Leary** is a Reach-Back Chemist at Federal Resources, in Stevensville, Maryland. **Brooke W. Kammrath** is an associate professor in the Forensic Science Department at the University of New Haven, in New Haven, Connecticut. Direct correspondence to: bkammrath@newhaven.edu

Aggregate and Fragment Analysis in Therapeutic Monoclonal Antibodies Using On-Line Size-Exclusion Chromatography with Native Mass Spectrometry

Aggregates and fragments are common product-related impurities in biopharmaceuticals that have impact on efficacy, safety, and stability. Identification of these low-level impurities may involve labor-intensive chromatographic fraction collection and follow-up experiments. In addition, a significant part of the total protein aggregates can be caused by non-covalent molecular interactions, which are dissociable in denaturing buffers, and cannot be characterized by conventional mass spectrometry (MS). With the use of ammonium acetate buffer, size-exclusion chromatography (SEC) can be coupled on-line to electrospray ionization MS for the characterization of size variants of therapeutical monoclonal antibodies (mAbs). A quadrupole time-of-flight (QTOF) MS system was employed, and the MS method was optimized to achieve favorable sensitivity for high-mass detection, while maintaining the structural integrity of the aggregates. As a result, high quality native MS spectra could be acquired for drug substance samples containing as low as 0.4% of these species, with the molecular masses of all relevant size variants obtained using 10-min SEC–MS runs. It is expected that this method will have significant potential to be implemented in routine analysis of mAbs for the characterization of the aggregation mechanisms and degradation pathways.

Chong-Feng Xu, Jing Xu, Zoran Sosic, and Bernice Yeung

Recombinant monoclonal antibodies (mAbs), as the most common modality among protein therapeutics, have achieved great success in multiple disease areas, including immunology, oncology, and blood diseases, and potentially could provide therapies for neurodegenerative diseases such as Alzheimer's disease (1–5). MAbs are large tetrameric molecules (approximately 146 kDa) composed of two heavy chains (~50 kDa) and two light chains (~23 kDa). The four chains are connected through interchain disulfide bonds. During manufacturing and storage, mAbs can form aggregates (or high molecular weight species [HMWs]) and fragments (or low molecular weight species [LMWs])(6). MAb aggregation can be formed through various mechanisms, such as molecular interactions and chemical cross-linking (6–9). The aggregates can be potentially immunogenic, and possibly promote the formation of particulates (10). MAb fragmentation can occur through several pathways, such as hydrolysis, free radical induced fragmentation, and enzymatic cleavage (11). The fragmented mAb may have reduced biological activity and pharmacokinetic compared to the intact mAb (12). Both aggregates and fragments are usually the critical quality attributes that need to be controlled to very low levels to ensure the efficacy, safety, and stability of mAb drugs.

Characterization of aggregates and fragments is important to understand mAb degradation pathways and to establish an effective control strategy. Conventional characterization methods

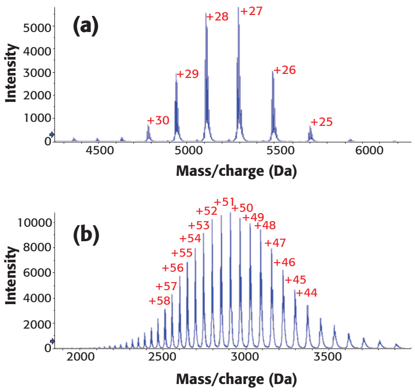

Figure 1: (a) Native and (b) denatured mass spectra of mAb-1 obtained on a QTOF instrument (Reprinted from a presentation slide of Sciex with permission).

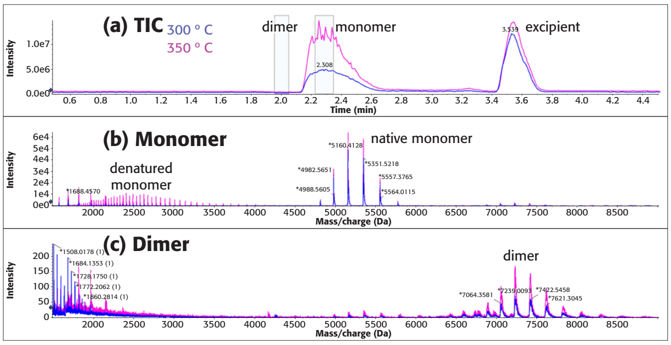

Figure 2: SEC-MS of mAb-2 with source temperature of 300 °C (blue trace) and 350 °C (purple trace). (a) total ion chromatogram (TIC); (b) Monomer mass spectrum; (c) Dimer mass spectrum.

often include size-exclusion chromatography (SEC) with UV or multi-angle light scattering (MALS) detection, analytical ultracentrifugation, and capillary electrophoresis with sodium dodecyl sulfate (6,7,9). In-depth characterization and identification of these low-level species may involve labor-intensive fraction collection and mass spectrometric analyses. In addition, noncovalent aggregates formed by molecular interactions can be a significant portion of the total aggregates, but are dissociable, and cannot be characterized by conventional denaturing liquid chromatography–mass spectrometry (LC–MS) methods (7, 9).

Native mass spectrometry has been an emerging technique in the past two decades for the study of protein complex assemblies (13,14), protein–protein interactions (15,16), protein–ligand interactions (15), glycoform analysis in mAbs (17,18), antibody–drug conjugates (19,20), bispecific antibodies (21), and mAb aggregates (22,23). For example, it has been specifically used for characterization of antibody–drug conjugates to determine the drug to antibody ratio (24,25), the study of product-related impurities and variants in bispecific antibodies (26), and study of aggregate formation in a coformulated drug containing two mAbs (27).

There are two special features of native MS: The need to use non-denaturing MS-compatible buffer and gentle ionization conditions to preserve protein complexes; and the need to use MS with high *m/z* ranges, because protein complexes have higher molecular weights, and are in native states carrying fewer charges compared to conventional denaturing states. In theory, time-of-flight (TOF) instruments have unlimited mass ranges, and thus are a natural fit for native MS. Some orbital ion trap instruments also have native MS capability, due to their extended mass ranges.

Apart from direct injection experiments, native MS can be coupled on-line to separation methods with the use of native or "near native" MS-compatible buffers, such as SEC (22,23,28), cation exchange chromatography (29), and capillary zone electrophoresis (30,31).

Early work in native MS has been described using a QTOF system (32). Recently, we used a TripleTOF QTOF instruments from Sciex to establish a native MS method for mAbs, and results are described in this paper. The method couples size-exclusion chromatography on-line with native MS using a MS-compatible SEC running buffer. The applications for the direct analysis of drug substance samples of therapeutic mAbs to obtain the molecular mass information of all the relevant size variants, including monomer, aggregates (in most cases the dimers), and fragments are demonstrated.

Materials and Methods

Antibodies

MAb-1 is the NIST mAb. MAb-2, mAb-3, mAb-4, and mAb-5 are humanized mAbs expressed in Chinese hamster ovary (CHO) cells at Biogen. For native SEC-MS analyses, the mAbs were diluted to final concentrations of 10 mg/mL using their formulation buffers.

Chemicals

Ammonium acetate (mass spectrometry grade) was purchase from Sigma. Milli Q water (18.2 MΩ) was used to prepare the ammonium acetate aqueous solutions.

Online Native SEC-MS Conditions

SEC separation was performed on a Shimadzu ultrahigh-pressure liquid chromatography (UHPLC) system with a Waters BEH200 SEC column (2.1 or 4.6 mm × 150 mm, 1.7-µm) heated to 30 °C. Typically, 50 or 100 µg mAb (50 µg for the 2.1 mm column; 100 µg for the 4.6 mm column) was loaded onto the column and eluted by a 25 mM ammonium acetate solution delivered at 100–200 µL/min (100 or 125 µL/min for the 2.1 mm column; 200 µL/min for the 4.6 mm column). The eluates were monitored sequentially by a PDA detector and a QTOF mass spectrometer.

Unless otherwise mentioned, the native MS data were acquired on a Sciex TripleTOF 6600 QTOF mass spectrometer, and the instrument parameters are summarized in

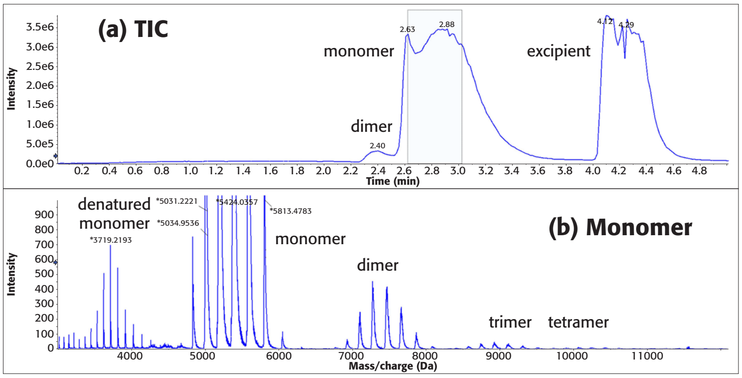

Figure 3: (a) TIC of native SEC-MS of mAb-3 under sample overloading conditions; (b) species detected in the monomer peak. Apart from the expected monomer signals, in-source artifacts including denatured monomer, dimer, trimer, and tetramer were observed at significantly lower levels.

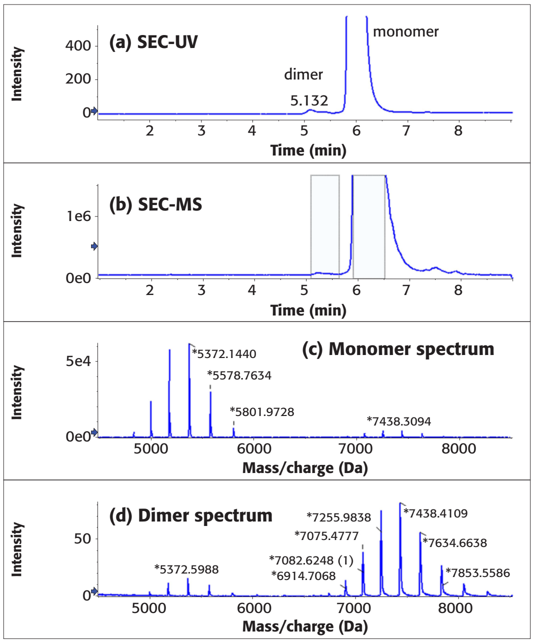

Figure 4: Native SEC-UV-MS of an mAb-4 drug substance sample. (a) UV chromatogram; (b) TIC chromatogram; (c) monomer mass spectrum; (d) dimer mass spectrum.

Table I. Data analysis was performed using PeakView 2.2 software (Sciex). Protein deconvolution was achieved using Bayesian algorithm in the Bio Tool Kit (Sciex).

Results and Discussion

Native and Denatured Mass Spectra of a Monoclonal Antibody

Shown in Figure 1 are the electrospray ionization mass spectra of mAb-1, acquired under native (Figure 1a) and denatured conditions (Figure 1b). In Figure 1b, as mAb-1 has been denatured by the organic solvent and the acidifier, more of the surface is exposed to the solvent, so that it takes on additional charges compared to the native state in a neutral aqueous solution (Figure 1a). As a result, the center charge states of the denatured and native mAb are 51 and 27, and their upper mass to charge ratio (*m/z*) ranges are approximately 4000 and 6000, respectively.

Moreover, the native mass spectrum appears to have a narrower charge state distribution, and reveals a simplified spectrum compared to the one under denaturing conditions. In the native spectrum, there are more spaces between nearby charge states, which increase the chance to detect and quantitate post-translational modifications when their signals fall in these regions. This could be a major reason that native MS has been increasingly popular for the analysis of antibody–drug conjugates (20).

Instrument Parameters for Native Mass Spectrometric Analysis of Monoclonal Antibodies

Native SEC–MS method optimization was based on the mass spectra of both the monomer and dimer peaks of mAbs after SEC separation on a 2.1 mm x 150 mm BEH200 column with 25 mM ammonium acetate buffer delivered at 0.125 mL/min. Multiple instrument parameters, including gas settings, source temperature, and declustering potential (DP) were evaluated. Right levels of source temperature and declustering potential are critical for removing solvent-related adducts and enhancing resolution and sensitivity. However, the excess levels of source temperature or declustering potential could induce denaturation and fragmentation of the analytes, which are not desirable.

Figure 2 shows the impact of source temperature on native SEC–MS analysis of mAb-2. Figure 2a shows the total ion chromatograms (TICs) under source temperature of 300 °C (blue trace) and 350 °C (purple trace), respectively. Two major analytes, the dimer and monomer, eluted at 2.0 min and 2.3 min, and their mass spectra are shown in Figure 2b and 2c, respectively. The MS signals of denatured monomer, native monomer, and dimer are in *m/z* windows of 1500–4000, 4500–6000, and 6500–8000, respectively. Compared to 300 °C, the higher source temperature doubled the sensitivity of the both the dimer and the monomer; however, it also denatured a significant portion of monomer. If we focus on dimer characterization, 350 °C could be chosen, otherwise, 300 °C or a temperature in between might be better choices to minimize monomer denaturation. Source temperature of 400 °C was also evaluated (data not shown). Under this elevated temperature, the recovery of dimer was not as good as that of 350 °C, since it became unstable and a portion of it decomposed into monomer and fragments.

SEC Separation is Critical for Native MS Analysis of MAb Dimer

In Figure 2b, there are a few low-level sig-

Table I: Optimized MS conditions for on-line native SEC-MS analysis of mAbs

Source Temperature, °C	Declustering Potential, eV	Collision Energy, eV	Ion Source Voltage, V	Ion Source Gas 1, psi	Ion Source Gas 2, psi	Curtain Gas, psi
275–375	100–130	6	5000	60	60	35
Script of Intact Protein Mode is on; Time-bins-to-sum: 80; *m/z* range: 3000–9000; Q1 transmission window: 100% at 2250 Da, Accumulation time, 1 s						

nals in the 6500–8500 *m/z* range, which align exactly to the mass spectrum of the dimer in Figure 2c. The dimer in Figure 2b was believed to be an artifact formed in-source. It can be postulated that, in direct injection experiments, the signals of artifactual in-source dimer could mask the signals of in-solution dimer. Therefore, SEC separation is beneficial in differentiating in-source dimer from in-solution dimer based on their different SEC retention times. Additionally, in direct injection experiments mAbs often need to be buffer-exchanged into mass-spectrometry compatible native buffers. During extended storage in native buffers, some mAbs may have a tendency toward concentration-dependent self-association, resulting in the formation of new aggregates that would not have been formed (or formed at much lower rates) when stored in formulation buffers. With native on-line SEC–MS, mAbs remain in their formulation buffers prior to injection, thus minimizing this risk.

Moreover, SEC provides separation and enrichment of the dimer peak, whose ionization could otherwise be suppressed by the monomer. The levels of dimer in drug substance samples are often very low, and so are their native MS signals. Overloading in SEC could be an approach used to enhance the signals of the dimer peaks. As shown in Figure 3a, 160 µg drug substance (DS) material, instead of a typical 50 µg material, was loaded on a 2.1 mm x 150 mm SEC column. Because the dimer is the first peak and a minor peak, overloading would not significantly impact its peak width and its separation from the monomer, and in theory the dimer response could be increased by approximately two- to threefold.

Shown in Figure 3b, however, in addition to the monomer peak, many in-source artifacts are also detected, such as the denatured monomer, dimer, trimer, and tetramer. Although these artifacts are undesirable, the detection of trimer and tetramer suggests that the TOF analyzer can cover a wide range of aggregates including but not limited to the dimer.

Sensitive Detection of MAb Dimer by Native SEC-MS

Even without sample overloading, the native SEC–MS method can achieve impressive sensitivity for the detection of mAb dimers. Shown in Figure 4, 100 µg DS sample of mAb-4 containing 0.4% dimer was analyzed by native SEC–UV-MS, with the use of a 4.6 mm x 150 mm SEC column. Figure 4a and 4b are the UV (280 nm) and TIC chromatograms of the DS sample, respectively. Figure 4c and 4d

Table II: Major species detected in mAb-5 by native SEC-MS

Protein	Theoretical Mass (Da)	Determined Mass (Da)	Mass Error (ppm)
Monomer (G0F/G0F)	145097	145125	193
Monomer (G0F/G1F)	145259	145288	200
Monomer (G1F/G1F)	145421	145451	206
Dimer (G0F/G0F/G1F/G1F)[a]	290518	290601	286
LMW (mAb - Fab)[b]	99358	99373	151

[a] Assuming that the glycoform in dimer is G0F/G0F/G1F/G1F (using a glycoform with median mass)

[b] Assuming that the glycoform in mAb-5 is G0F/G1F (using a glycoform with median mass), and cleavage is between the K and T in hinge sequence "CD**K**THT" (cleavage in the middle of the sequence) (33). The cleavages can be anywhere in the hinge sequence, and the LMW is likely a complex mixture of proteins with similar masses.

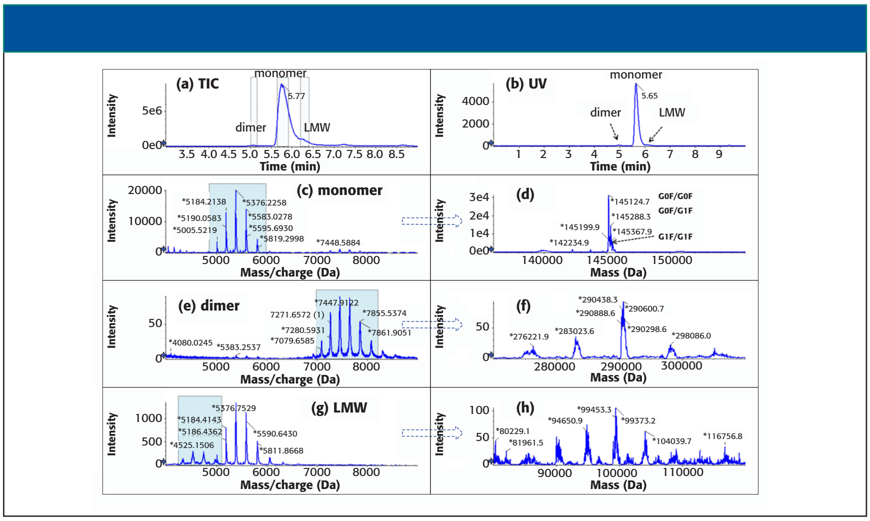

Figure 5: Native SEC–UV/MS of a mAb-5 drug substance sample. (a) TIC chromatogram; (b) UV chromatogram; (c), (e) and (g): raw mass spectra of the monomer, dimer and LMW peak, respectively; (d), (f) and (h): deconvoluted mass spectra of adjacent peaks (to the left in column one).

are the mass spectra of the monomer and dimer, respectively.

The 0.4 µg dimer on column generated a high-quality native mass spectrum with base peak intensity of approximately 80 (Figure 4d). From these data, it is likely that this SEC–MS method could be applied to a DS sample containing 0.1% dimer. The 0.1 ug (0.1%) dimer from 100 µg DS would generate a mass spectrum with base peak intensity of approximately 20, which is close to the quantitation limit (10–20 ion counts) of the mass detector.

MAb Size Variant Characterization by Native SEC-MS

Size variants, including aggregates and fragments, are product-related impurities that are critical to the quality of protein drugs. Characterization of size variants is important for the understanding of the stability profiles and degradation pathways in the mAbs.

To analyze the size variants in mAb-5, 100 µg of DS sample containing 1.6% dimer was analyzed by the native SEC–UV-MS method (Figure 5). Three major peaks were detected, including the monomer, dimer, and a low molecular weight (LWM) peak. Their raw mass spectra and deconvoluted mass spectra are shown in Figure 5c, 5e, 5g, and Figure 5d, 5f, 5h, respectively.

In Figure 5d, the deconvoluted native mass spectrum supports the identification of major glycoforms of mAb-5. Deconvoluted mass spectrum of the dimer is shown in Figure 5f. Deconvoluted mass spectrum of the LMW-containing mAb missing a single Fab due to commonly observed hinge cleavage is shown in Figure 5h (33). The mass accuracies are generally about 200 ppm (Table II), which are typically considered to be low but acceptable for the purpose of analysis presented here. For the dimer and LMW species, due to their low abundances and high levels of heterogeneities, the deconvoluted spectra (Figure 5f and 5h) contain a few additional harmonic peaks. It appears that the deconvolution algorithm has not been fully optimized for native spectra analysis. Nevertheless, the base peaks in the deconvoluted spectra accurately report the molecular masses of these analytes.

The assignments of the glycoforms in the monomer, as well as the identification of dimer and LMW peaks, are summarized in Table II. From this data, all the major size variants in the mAb-5 DS sample can be identified using a 10-min native SEC–MS run.

Conclusion

Native SEC–MS conditions were optimized for the analysis of mAb size variants, with the use of ammonium acetate SEC buffer and a TOF mass spectrometer. This method is fast and sensitive for direct size variant characterization of mAbs at levels as low as 0.4%. The method was successfully applied to characterize all the relevant size variants detected in various mAbs. Native SEC–MS has been demonstrated to be a useful technique for mAb aggregate characterization. It has significant potential to be routinely applied to study mAb aggregation mechanisms and degradation pathways, thus provides valuable information to guide purification and formulation process development, and supports the risk assessment of product-related impurities.

Acknowledgment

The authors thank Sean McCarthy, Fan Zhang, Esme Candish, and Elliott Jones at Sciex for the technical support of this work.

References

(1) M. Trikha, L. Yan, and M.T. Nakada, *Curr. Opin. Biotechnol.* **13,** 609–614 (2002).
(2) A.L. Nelson, E. Dhimolea, and J.M. Reichert, *Nat. Rev. Drug Discov.* **9,** 767–774 (2010).

Continued on Page 24

The 2020 ASMS Conference Moved On-line in a Comprehensive Format

John Chasse

Faced with the COVID-19 pandemic, the American Society for Mass Spectrometry (ASMS) Board canceled the face-to-face ASMS Conference on Mass Spectrometry & Allied Topics, originally scheduled for May 31 to June 4 in Houston, Texas, and announced that they would shift the program to an on-line format. “Although the program would be delivered in a new and different manner, we remain committed to hosting and sharing brilliant science for a re-imagined ASMS 2020,” Richard A. Yost, the ASMS president, said in a statement.

With the event redubbed “The ASMS 2020 Reboot,” talks and posters will be presented in a virtual and interactive format using the familiar on-line planner and mobile app tools used at the annual conference in past years, with a schedule as follows:

- On-demand videos of orals will begin on June 1.
- Poster PDFs and optional poster presentation videos will also begin on that date.
- Live webinars will be conducted for plenary lectures, tutorials, award lectures, and presentations, approximately 50 workshops, with live question-and-answer (Q&A) sessions for each of the planned 64 oral sessions, and the annual ASMS meeting (including board updates and additional award presentations.) These live webinars will be scheduled Monday–Friday, June 1–5 and June 8–12, from 10:00 am to 3:00 pm+ Central Daylight Time (CDT) on most of these days. Optional one hour Corporate Member activities will be held at start and end of each day.
- The live webinars will be in the format of a “watch party” of each oral session (6 talks) followed by live Q&A with speakers. Attendees may also watch the talks individually on-demand at any time beginning June 1, but still join any Q&A at the scheduled times during the week of June 8.

Highlights of the Conference are outlined below.

Monday, June 1

- Two tutorials will be conducted. From 12:30 to 1:15 pm CDT, “Single-Cell Mass Spectrometry” will be presented by Peter Nemes of the University of Maryland, College Park, and from 1:30 pm to 2:15, “Glycoprotein Analysis for Understanding Human Disease” will be presented by Heather Desaire of the University of Kansas.
- A special keynote lecture, “Is There Still Gender Bias in Academic Science (and Does It Matter)? What the Scientific Studies Say,” will be delivered by Corinne Moss-Racusin from Skidmore College from 1:30 to 2:15 pm CDT.
- From 2:30 to 3:30 pm CDT, the Opening Plenary Lecture, “Mars 2020,” will be delivered by Patricia M. Beauchamp, the Chief Technologist of the Engineering and Science Directorate,at the Jet Propulsion Laboratory of the California Institute of Technology.
- From 9:00 to 10:00 am and again from 3:00 to 4:00 pm CDT, there will be featured corporate member activities, including on-line seminars, product launches, and demonstrations

Tuesday, June 2

- The first 16 of 56 webinar-style workshops will be conducted by interest groups or independent organizers, in two sessions, with workshops 1–8 held concurrently from 10:00 to 11:30 am CDT, and workshops 9–16 held concurrently from 12:00 to 1:30 pm CDT. This schedule will continue with 16 workshops per day, Tuesday through Thursday, with 8 on Friday.
- From 1:45 to 3:15 CDT, The Al Yergey MS Scientist Award will be presented to Rachel Ogorzalek, a research biological chemist at UCLA. This will be followed by the Award Lecture for the John B. Fenn Distinguished Contribution in Mass Spectrometry Award, presented by Michael L. Gross, of Washington University in St. Louis, Missouri.
- Corporate events will be held 9:00–10:00 am and 3:15–4:15 pm.

Wednesday, June 3

- From 1:45 to 3:15 pm CDT, Research Awards will be presented to Jace Jones of the University of Maryland, Miklos Guttman of the University of Washington, and Ian K. Webb of Indiana University and Purdue University. Also, the Research at Primarily Undergraduate Institutions (PUIs) Award will be presented to Christine Hughey of James Madison University in Harrisonburg, Virginia, and the Biemann medal will be presented to Ying Ge, a Professor of Cell and Regenerative Biology and Chemistry at the University of Wisconsin at Madison.
- Workshops 17–24 and 25–32 will be held from 10:00 to 11:30 am and 12:00 to 1:30 pm CDT.
- Corporate events will be held 9:00–10:00 am and 3:15–4:15 pm.

Thursday, June 4

- From 2:00 to 3:30 pm CDT, awards for Postdoctorate Career Development will be presented to Juan Aristizabal Henao of the University of Florida in Gainesville, Florida, Wout Bittremieux of the University of California–San Diego, Kevin Clark of the Beckman Institute for Advanced Science and Technology (part of the University of Illinois at Urbana-Champaign), Kelly Karch of

Image credit: Used with permission from the American Society for Mass Spectrometry

the Ohio State University, and Lindsay Pino of the University of Pennsylvania. In addition, the Ron Hites Award for Outstanding JASMS Publication will be presented to Stephen J. Valentine of West Virginia University and his co-authors Samaneh Ghassabi Kondalaji and Mahdiar Khakinejad for their paper, “Comprehensive Peptide Ion Structure Studies Using Ion Mobility Techniques: Part 3. Relating Solution-Phase to Gas-Phase Structures.”

- Workshops 33–40 and 41–48 will be held from 10:00 to 11:30 am and 12:00 to 1:30 pm CDT.

Friday, June 5

- The ASMS plans a 4-hour virtual “exhibit hall” from 12:00 to 4:00 pm CDT. This will be a specific timeframe when the society encourages all registrants of the Reboot to peruse exhibitor listings in the mobile app or on-line planner. ASMS corporate members are encouraged to host their own chat room or event during this period. Registrants can look for links within each Corporate Member or Exhibitor listing in the mobile app or on-line planner.

Monday, June 8–Thursday, June 11

- From Monday through Thursday of the second week of the conference, two groups of oral sessions (eight sessions conducted in parallel in each) will be conducted from 10:00 am to 12 noon and from 1:15 to 3:15 pm CDT.
- These oral presentations will be followed by live Q&A periods from 12:15 pm to 1:00 pm and 3:30 to 4:15 pm, respectively, with one Q&A period covering the six talks in each oral session. Registrants may submit questions via the on-line planner or mobile app. Attendees may also watch the talks individually on-demand at any time beginning June 1, but still join any Q&A at the scheduled times during the week of June 8.

Friday, June 12

- From 10:00 to 11:00 am CDT, Stephen Brusatte of the University of Edinburgh will give the closing plenary lecture, “New Dinosaur Discoveries.”

The deadline to register is May 22. The society hopes to offer late registration at increased fees, but, as we go to press, they are not certain that this will be an option. On-demand content will remain available to registrants through August 31.

More information, including on-line event schedules, can be found at https://asms.org/conferences/asms-2020-reboot.

John Chasse is the Managing Editor of *Spectroscopy* and *LCGC North America.* Direct correspondence to JChasse@MJHLifeSciences.com.

Continued from Page 22

References

(3) N.A.P.S. Buss, S.J. Henderson, M. McFarlane, J.M. Shenton, and L. de Haan, *Curr. Opin. Pharmacol.* **12,** 615–622 (2012).

(4) Y.J. Yu and R.J. Watts. *Neurotherapeutics* **10,** 459–472 (2013).

(5) J. Sevigny, P. Chiao, T. Bussière, P.H. Weinreb, L. Williams, M. Maier, R. Dunstan, S. Salloway, T. Chen, Y. Ling, J. O’Gorman, F. Qian, M. Arastu, M. Li, S. Chollate, M.S. Brennan, O. Quintero-Monzon, R.H. Scannevin, H.M. Arnold, T. Engber, K. Rhodes, J. Ferrero, Y. Hang, A. Mikulskis, J. Grimm, C. Hock, R.M. Nitsch, and A. Sandrock, *Nature* **537,** 50–56 (2016).

(6) A. Beck, E. Wagner-Rousset, D. Ayoub, A. Van Dorsselaer, and S. Sanglier-Cianférani, *Anal. Chem.* **85,** 715–736 (2013).

(7) M. Vázquez-Rey and D.A. Lang, *Biotechnol. Bioeng.* **108,** 1494–1508 (2011).

(8) C.-F. Xu, Y. Chen, L. Yi, T. Brantley, B. Stanley, Z. Sosic, and L. Zang, *Anal. Chem.* **89,** 7915–7923 (2017).

(9) C.J. Roberts, *Trends Biotechnol.* **32,** 372–380 (2014).

(10) K.D. Ratanji, J.P. Derrick, R.J. Dearman, and I. Kimber, *J. Immunotoxicol.* **11,** 99–109 (2014).

(11) J. Vlasak and R. Ionescu, *mAbs* **3,** 253–263 (2011).

(12) A.L. Nelson and J. M. Reichert, *Nat. Biotechnol.* **27,** 331–337 (2009).

(13) R.H.H. v.d. Heuvel and A.J.R. Heck, *Curr. Opin. Chem. Biol.* **8,** 519–526 (2004).

(14) M. Sharon and C.V. Robinson, *Annu. Rev. Biochem.* **76,** 167–193 (2007).

(15) A.J.R. Heck and R.H.H. v.d. Heuvel, *Mass Spectrom. Rev.* **23,** 368–389 (2004).

(16) A.J.R. Heck, *Nat. Methods* **5,** 927–933 (2008).

(17) S. Rosati, Y. Yang, A. Barendregt, and A.J.R. Heck, *Nat. Protoco.* **9,** 967–976 (2014).

(18) S. Rosati, E.T.J. v.d. Bremer, J. Schuurman, P.W.H.I. Parren, JP. Kamerling, and A.J.R. Heck, *mAbs* **5,** 917–924 (2013).

(19) R.Y.C. Huang and G. Chen, *Drug Discov. Today* **21,** 850–855 (2016).

(20) A. Beck, V. D’Atri, A. Ehkirch, S. Fekete, O. Hernandez-Alba, R. Gahoual, E. Leize-Wagner, Y. François, D. Guillarme, and S. Cianférani, *Expert Rev. Proteomic.* **16,** 337–362 (2019).

(21) G. Terral, A. Beck, and S. Cianférani, *J. Chromatogr. B* **1032,** 79–90 (2016).

(22) B. Kükrer, V. Filipe, E. van Duijn, P.T. Kasper, R.J. Vreeken, A.J.R. Heck, and W. Jiskoot, *Pharm. Res.* **27,** 2197–2204 (2010).

(23) M. Haberger, M. Leiss, A.-K. Heidenreich, O. Pester, G. Hafenmair, M. Hook, L. Bonnington, H. Wegele, M. Haindl, D. Reusch, and P. Bulau, *mAbs* **8,** 331–339 (2016).

(24) J. Chen, S. Yin, Y. Wu, and J. Ouyang, *Anal. Chem.* **85,** 1699–1704 (2013).

(25) F. Debaene, A. Bœuf, E. Wagner-Rousset, O. Colas, D. Ayoub, N. Corvaïa, A. Van Dorsselaer, A. Beck, and S. Cianférani, *Anal. Chem.* **86,** 10674–10683 (2014).

(26) Y.-T Yan, T. Xing, S.-H. Wang, T.J. Daly, and N. Li, *Anal. Chem.* **91,** 11417–11424 (2019).

(27) T. Xing, Y.-T. Yan, S.-H. Wang, T J. Daly, and N. Li, “Identification and quantitation of heterodimer species in co-formulated protein drugs by lc-ms-based approaches” 67TH ASMS Conference on Mass Spectrometry and Allied Topics; June 6th; Atlanta, Georgia 2019.

(28) K. Muneeruddin, J.J. Thomas, P.A. Salinas, and I.A. Kaltashov, *Anal. Chem.* **86,** 10692–10699 (2014).

(29) Y. Leblanc, V. Faid, M.A. Lauber, Q. Wang, N. Bihoreau, and G. Chevreux, *J. Chromatogr. B* **1133,** 121814 (2019).

(30) A.M. Belov, R. Viner, M.R. Santos, D.M. Horn, M. Bern, B.L. Karger, and A.R Ivanov, *J. Am. Soc. Mass Spectrom.* **28,** 2614–2634 (2017).

(31) E.A. Redman, J.S. Mellors, J.A. Starkey, and J.M. Ramsey, *Anal. Chem.* **88,** 2220–2226 (2016).

(32) N.J. Thompson, S. Rosati, and A.J.R. Heck, *Methods* **65,** 11–17 (2014).

(33) C-F. Xu, L. Zang, and A. Weiskopf, *J. Chromatogr. B* **960,** 230–238 (2014).

Chong-Feng Xu, Jing Xu, Zoran Sosic, and Bernice Yeung are with the Department of Analytical Development at Biogen, in Cambridge, Massachussetts. Direct correspondence to chongfeng.xu@biogen.com

Characterization of a TSKgel® FcR-IIIA-NPR™ HPLC Column by Top-Down Mass Spectrometry

Tosoh Bioscience

Monoclonal antibodies (mAbs) comprise the largest class of glycosylated protein therapeutics currently on the market, and glycosylation is known to be a major source of mAb heterogeneity. N-glycosylation of IgG-Fc of mAbs is known to impact drug therapeutic mechanism of action (MOA), thus monitoring glycan critical quality attributes (CQAs) is an essential part of biopharmaceutical development. Glycosylation is a critical factor in drug product solubility, kinetics, stability, efficacy, and immunogenicity. Analytical methods utilize a suite of chromatographic modes using high performance liquid chromatography (HPLC) to analyze glycosylation of both intact and digested protein molecules.

The TSKgel FcR-IIIA-NPR (non-porous resin) column is a high-performance affinity chromatography column for the analysis of IgG glycoforms. The stationary phase utilizes a recombinant FcR-IIIA protein bound to a nonporous polymethacrylate polymer. The retention mechanism is based on the interaction between the FcR ligand and the sugar moieties attached to the asparagine (ASN) amino acid in the conserved region of the monoclonal antibody. The resulting elution profile of the glycoprotein mimics antibody-dependent cellular cytotoxicity (ADCC activity), which is correlated to the composition of the N-glycans.

The purpose of this study is to demonstrate the use of mass spectrometry to characterize the elution profile of a typical IgG_1 molecule separation on a TSKgel FcR-IIIA-NPR column, and verify the observations that certain glycan structures impart higher activity to the monoclonal antibody, especially as it relates to the presence of terminal galactose sugars.

Experimental HPLC Conditions

TSKgel FcR-IIIA-NPR Separation

Column:	TSKgel FcR-IIIA-NPR, 5 µm, 4.6 mm ID × 7.5 cm
Instrument:	Agilent 1200
Mobile phase:	A: 50 mmol/L Na citrate, pH 6.5 B: 50 mmol/L Na citrate, pH 4.5
Gradient:	0 min: 0% B, 20 min: 100% B, 30 min, 100% B
Flow rate:	0.85 mL/min
Detection:	UV @ 280 nm, 25 Hz
Temperature:	15 °C
Injection vol.:	5 µL
Sample:	NIST mAb fractions; 5 mg/mL in mobile phase A

Top-Down MS Characterization

Column:	TSKgel Protein C4-300, 3 µm, 2.0 mm ID × 15 cm
Instrument:	Shimadzu Nexera® XR
Mobile phase:	A: 0.1% formic acid in water B: 0.1% formic acid in acetonitrile
Gradient:	0 min: 10% B, 40 min: 95% B, 50 min: 95% B
Flow rate:	0.2 mL/min
Detection:	Sciex X500B Q-TOF, ESI positive, m/z 900–4000
Temperature:	50 °C
Injection vol.:	5 µL
Samples:	NIST mAb fractions; 100 µg/mL in LC–MS water

MS conditions

Source gas 1	50 psi	Spray voltage	**5000eV**
Source gas 2	50 psi	Declustering potential	250 eV
Curtain gas	50 psi	DP spread	0 eV
CAD gas	7 psi	Collision energy	10 eV
Source temp	400 °C	CE spread	0 eV
Accumulation time	1 sec	Bins to sum	80

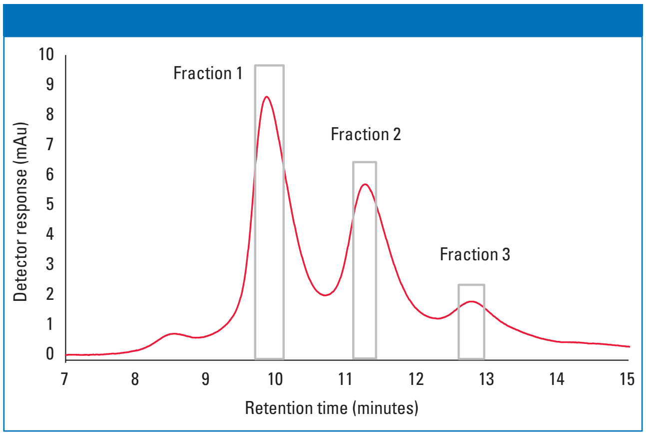

Figure 1: Zoomed view of the elution profile of NIST mAb on TSKgel FcR-IIIA-NPR. The boxes highlighting each peak represent fractions that were collected.

Results and Discussion

Figure 1 demonstrates the separation of NIST mAb on the TSKgel FcR-IIIA-NPR column. IgG_1 molecules yield this typical type of elution profile based on glycoform composition that is consistent with ADCC activity. This offers a fast orthogonal chromatographic method for determination of antibody activity and comparisons of antibody heterogeneity.

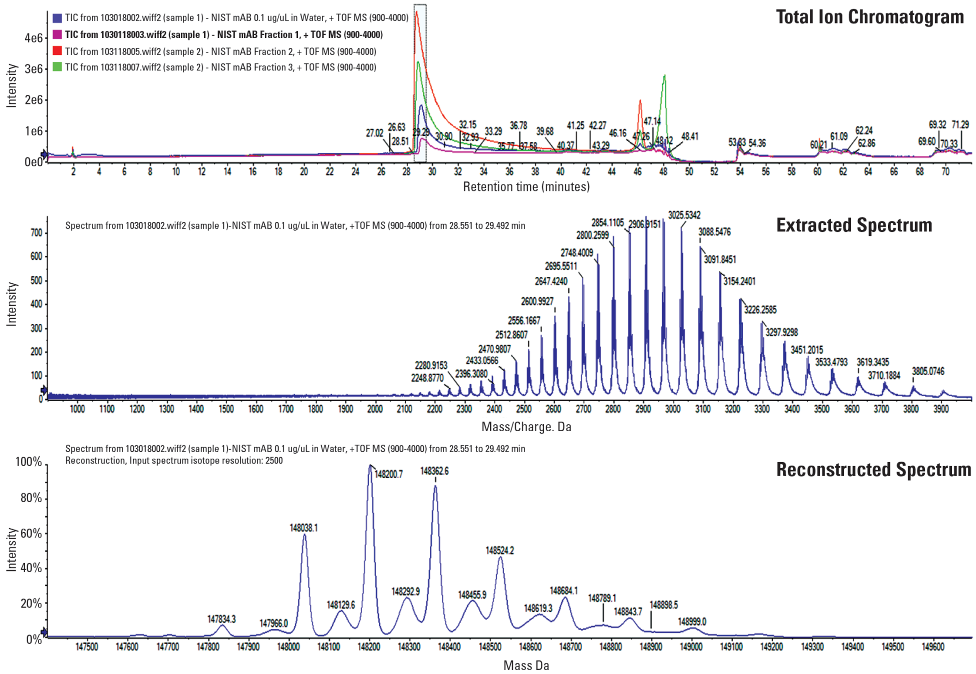

Figure 2: The TIC, extracted spectrum, and reconstructed spectrum for a NIST mAb control sample. The glycoforms observed for this sample are in agreement with accepted literature on characterization of this molecule.

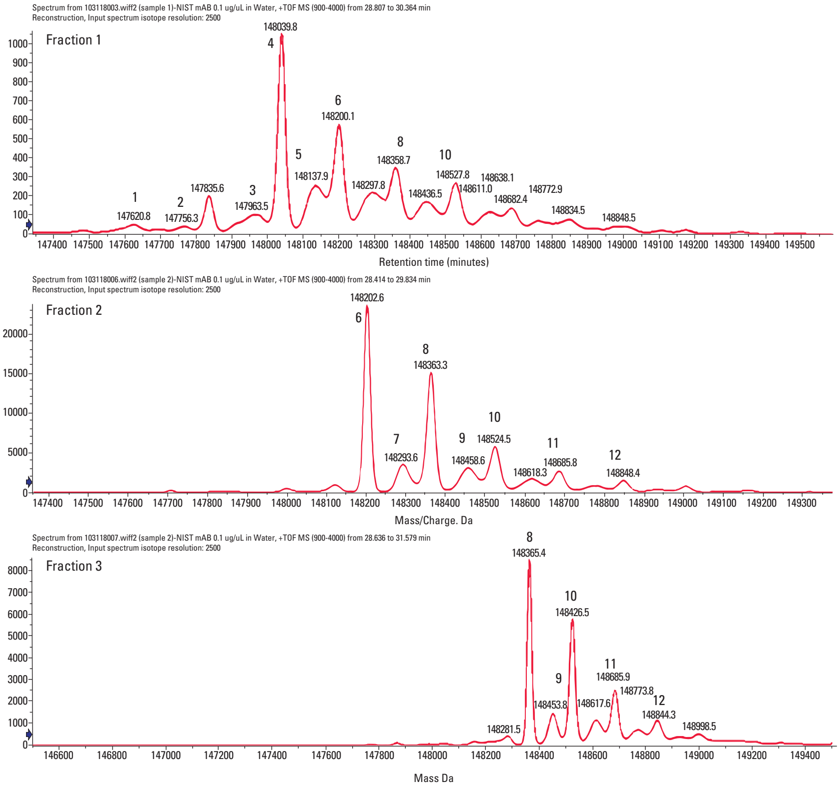

Figure 3: Reconstructed spectra for each of the isolated peak fractions, indicating that later eluting fractions have a greater proportion of terminal galactose glycan sugars, consistant with observations of antibody activity and percentage of galactose.

Data for isolated peak fractions in reconstructed spectra (Figure 3)

Peak	Mass	Spray voltage	Peak	Mass	Glycoform
1	147620	GOF/GOF (-2Glc NAc)	7	148292	GOF/G1F (Adduct)
2	147756	GOF/GOF (-Glc NAc)	8	148362	G1F/G1F
3	147966	GOF/G1F (-Glc NAc)	9	148455	G1F/G1F (Adduct)
4	148038	GOF/GOF	10	148524	GOF/G2F (+Hex)
5	148129	GOF/GOF (Adduct)	11	148684	G2F/G2F (+Hex)
6	148200	GOF/G1F	12	148843	G2F/G2F

The three largest eluting peaks were collected and analyzed by offline mass spectrometry. Peak fractions were pooled from successive 25 µg on column injections, concentrated, and buffer exchanged to liquid chromatography–mass spectrometry (LC–MS)-grade water.

Figures 2 and 3 illustrate analysis of the NIST mAb standard compared against the collected peak fractions. It is observed that each peak has a unique composition of intact mAb glycoforms, and that the selectivity of the stationary phase is based on the amount of terminal galactose units on the glycan moiety. This conclusion agrees with studies that show antibodies with higher amounts of G1- and G2-containing sugars show greater ADCC activity. Because of some peak overlap in the initial separation, there is some overlap of different galactose-containing species in the MS profile, though the general trend between galactose and activity has been confirmed.

Conclusions

The separation of an IgG_1 molecule was demonstrated using the TSKgel FcR-IIIA-NPR column and peaks from that separation were characterized by high-resolution mass spectrometry. The results support that the stationary phase selectivity is based on the same Fc-glycan/Fc receptor interaction as ADCC activity. The glycoform composition of each peak is consistent with previous published observations on the activity of N-glycan sugars with higher amounts of terminal galactose.

This application demonstrates the efficacy of this approach and characterization data that demonstrate the proof of concept of this chromatographic technique for a fast orthogonal analysis to evaluate mAb ADCC activity, potentially for early cell line development, bioreactor modeling, and lot-to-lot comparability of therapeutic antibodies.

Tosoh Bioscience and TSKgel are registered trademarks of Tosoh Corporation.

NPR is a registered trademark of Tosoh Corporation in Japan, EU, China, and India.

Nexera is a registered trademark of Shimadzu Corporation.

TOSOH

TOSOH BIOSCIENCE

Tosoh Bioscience LLC
3604 Horizon Drive, Suite 100, King of Prussia, PA 19406
tel. (484) 805-1219, fax (610) 272-3028
Website: www.tosohbioscience.com

Analysis of Fentanyl and Its Analogues in Human Urine by LC–MS/MS

Shun-Hsin Liang and Frances Carroll, Restek Corporation

Abuse of synthetic opioid prescription painkillers such as fentanyl, along with a rapidly growing list of illicit analogues, is a significant public health problem. In this study, we developed a simple dilute-and-shoot method that provides a fast 3.5-min analysis of fentanyl and related compounds (norfentanyl, acetyl fentanyl, alfentanil, butyryl fentanyl, carfentanil, remifentanil, and sufentanil) in human urine by liquid chromatography–tandem mass spectrometry (LC–MS/MS) using a Raptor Biphenyl column.

In recent years, the illicit use of synthetic opioids has skyrocketed, and communities worldwide are now dealing with an ongoing epidemic. Of the thousands of synthetic opioid overdose deaths per year, most are related to fentanyl and its analogues. With their very high analgesic properties, synthetic opioid drugs such as fentanyl, alfentanil, remifentanil, and sufentanil are potent painkillers that have valid medical applications; however, they are also extremely addictive and are targets for abuse. In addition to abuse of these prescription drugs, the current opioid crisis is fueled by a growing number of illicit analogues, such as acetyl fentanyl and butyryl fentanyl, which have been designed specifically to evade prosecution by drug enforcement agencies.

As the number of opioid drugs and deaths increases, so does the need for a fast, accurate method for the simultaneous analysis of fentanyl and its analogues. Therefore, we developed this LC–MS/MS method for measuring fentanyl, six analogues, and one metabolite (norfentanyl) in human urine. A simple dilute-and-shoot sample preparation procedure was coupled with a fast (3.5 min) chromatographic analysis using a Raptor Biphenyl column. This method provides accurate, precise identification, and quantitation of fentanyl and related compounds, making it suitable for a variety of testing applications, including clinical toxicology, forensic analysis, workplace drug testing, and pharmaceutical research.

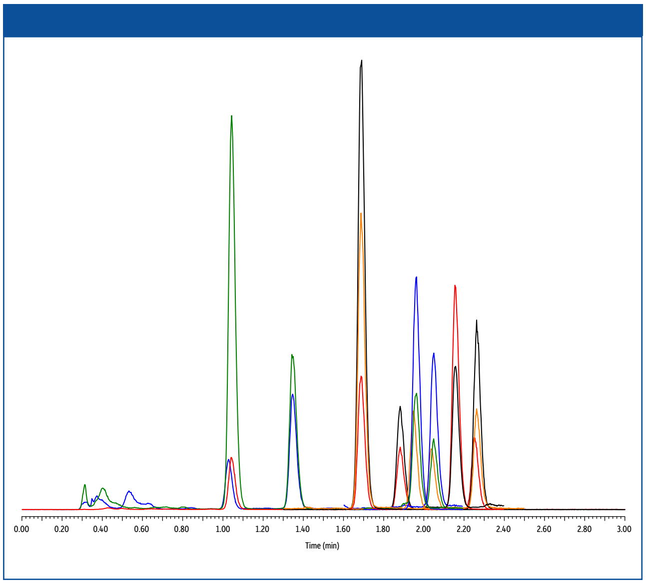

Figure 1: The Raptor Biphenyl column effectively separated all target compounds in urine with no observed matrix interferences. Peak elution order: norfentanyl-D_5, norfentanyl, remifentanil, acetyl fentanyl-$^{13}C_6$, acetyl fentanyl, alfentanil, fentanyl-D_5, fentanyl, carfentanil-D_5, carfentanil, butyryl fentanyl, sufentanil-D_5, sufentanil.

Experimental Conditions

Sample Preparation

The analytes were fortified into pooled human urine. An 80 µL urine aliquot was mixed with 320 µL of 70:30 water–methanol solution (fivefold dilution) and 10 µL of internal standard (40 ng/mL in methanol) in a Thomson SINGLE StEP filter vial (Restek cat. #25895). After filtering through the 0.2 µm PVDF membrane, 5 µL was injected into the LC–MS/MS.

Table I: Analyte transitions

Analyte	Precursor Ion	Product Ion Quantifier	Product Ion Qualifier	Internal Standard
Norfentanyl	233.27	84.15	56.06	Norfentanyl-D_5
Acetyl fentanyl	323.37	188.25	105.15	Acetyl fentanyl-$^{13}C_6$
Fentanyl	337.37	188.26	105.08	Fentanyl-D_5
Butyryl fentanyl	351.43	188.20	105.15	Carfentanil-D_5
Remifentanil	377.37	113.15	317.30	Norfentanyl-D_5
Sufentanil	387.40	238.19	111.06	Sufentanil-D_5
Carfentanil	395.40	113.14	335.35	Carfentanil-D_5
Alfentanil	417.47	268.31	197.23	Acetyl fentanyl-$^{13}C_6$
Norfentanyl-D_5	238.30	84.15	—	—
Acetyl fentanyl-$^{13}C_6$	329.37	188.25	—	—
Fentanyl-D_5	342.47	188.27	—	—
Sufentanil-D_5	392.40	238.25	—	—
Carfentanil-D_5	400.40	340.41	—	—

Calibration Standards and Quality Control Samples

The calibration standards were prepared in pooled human urine at 0.05, 0.10, 0.25, 0.50, 1.00, 2.50, 5.00, 10.0, 25.0, and 50.0 ng/mL. Three levels of QC samples (0.75, 4.0, and 20 ng/mL) were prepared in urine for testing accuracy and precision with established calibration standard curves. Recovery analyses were performed on three different days. All standards and QC samples were subjected to the sample preparation procedure described.

LC–MS/MS analysis of fentanyl and its analogues was performed on an ACQUITY UPLC instrument coupled with a Waters Xevo TQ-S mass spectrometer. Instrument conditions were as follows, and analyte transitions are provided in Table I.

Analytical column:	Raptor Biphenyl (5 µm, 50 mm × 2.1 mm; cat. #9309552)	
Guard column:	Raptor Biphenyl EXP guard column cartridge, (5 µm, 5 mm × 2.1 mm; cat. #930950252)	
Mobile phase A:	0.1% Formic acid in water	
Mobile phase B:	0.1% Formic acid in methanol	
Gradient	Time (min)	%B
	0.00	30
	2.50	70
	2.51	30
	3.50	30
Flow rate:	0.4 mL/min	
Injection volume:	5 µL	
Column temp.:	40 °C	
Ion mode:	Positive ESI	

Results

Chromatographic Performance

All eight analytes were well separated within a 2.5-min gradient elution (3.5-min total analysis time) on a Raptor Biphenyl column (Figure 1). No significant matrix interference was observed to negatively affect quantification of the fivefold diluted urine samples. The 5-µm particle Raptor Biphenyl column used here is a superficially porous particle (SPP) column. It was selected for this method in part because it provides similar performance to a smaller particle size fully porous particle (FPP) column, but it generates less system back pressure.

Linearity

Linear responses were obtained for all compounds and the calibration ranges encompassed typical concentration levels monitored for both research and abuse. Using 1/x weighted linear regression ($1/x^2$ for butyryl fentanyl), calibration linearity ranged from 0.05 to 50 ng/mL for fentanyl, alfentanil, acetyl fentanyl, butyryl fentanyl, and sufentanil; from 0.10 to 50 ng/mL for remifentanil; and from 0.25 to 50 ng/mL for norfentanyl and carfentanil. All analytes showed acceptable linearity with r^2 values of 0.996 or greater and deviations of <12% (<20% for the lowest concentrated standard).

Accuracy and Precision

Based on three independent experiments conducted on multiple days, method accuracy for the analysis of fentanyl and its analogues was demonstrated by the %recovery values, which were within 10% of the nominal concentration for all compounds at all QC levels. The %RSD range was 0.5–8.3% and 3.4–8.4% for intraday and interday comparisons, respectively, indicating acceptable method precision (Table II).

Conclusions

A simple dilute-and-shoot method was developed for the quantitative analysis of fentanyl and its analogues in human urine. The analytical method was demonstrated to be fast, rugged, and sensitive with acceptable accuracy and precision for urine sample analysis. The Raptor Biphenyl column is well suited for the analysis of these synthetic opioid compounds, and this method can be applied to clinical toxicology, forensic analysis, workplace drug testing, and pharmaceutical research.

RESTEK
Pure Chromatography

Restek Corporation
110 Benner Circle, Bellefonte, PA 16823
tel. 1 (814) 353-1300
Website: www.restek.com

Table II: Accuracy and precision results for fentanyl and related compounds in urine QC samples

	QC Level 1 (0.750 ng/mL)			QC Level 2 (4.00 ng/mL)			QC Level 3 (20.0 ng/mL)		
Analyte	**Average Conc. (ng/mL)**	**Average % Accuracy**	**%RSD**	**Average Conc. (ng/mL)**	**Average % Accuracy**	**%RSD**	**Average Conc. (ng/mL)**	**Average % Accuracy**	**%RSD**
Acetyl fentanyl	0.761	102	1.54	3.99	99.7	2.08	19.9	99.3	0.856
Alfentanil	0.733	97.6	3.34	3.96	98.9	8.38	20.9	104	6.73
Butyryl fentanyl	0.741	98.9	6.29	3.77	94.3	6.01	20.8	104	4.95
Carfentanil	0.757	101	7.34	3.76	94.0	4.64	20.6	103	4.24
Fentanyl	0.761	102	1.98	3.96	99.1	2.31	19.9	99.6	1.04
Norfentanyl	0.768	103	6.50	4.04	101	1.84	20.1	101	2.55
Remifentanil	0.765	102	3.42	3.97	99.2	3.68	20.8	104	4.14
Sufentanil	0.752	100	1.67	3.93	98.3	1.28	20.1	100	0.943

Shodex HILICpak VC-50: Unique Multimodal Column for Polar Anionic Substances Including Neurotransmitter Analysis

Showa Denko America, Inc.

Neurotransmitters are chemical messengers that transmit signals across a chemical synapse from the neuron by binding to specific receptors. Many neurotransmitters are synthesized from amino acids, and only require a small number of biosynthetic steps for conversion. Neurotransmitters can range from about the size of a single amino acid to a large protein. Since they are composed primarily of amino acids, a column with diol-functional groups would be ideal to analyze samples containing neurotransmitters. Due to their structure, carboxyl functionalize packing material is an ideal-need diol group to analyze by high-performance liquid chromatography (HPLC) analysis.

Shodex introduces the HILICpak VN-50 series with neutral carboxyl-type PVA-based hydrophilic interaction liquid chromatography (HILIC) solid supports. The packing material is more rugged than similar zwitterion-type columns, but easier to handle and equilibrate. This series can be used for traditional HPLC and liquid chromatography–mass spectrometry (LC–MS) applications and is shown to analyze neurotransmitters.

Here, five neurotransmitters were analyzed using the HILICpak VC-50 2D with MS.

Experimental Conditions

A sample containing five monoamine neurotransmitters—noradrenaline, adrenaline, dopamine, serotonin, and histamine—was analyzed using a Shodex HILICpak VN-50 2D (2.0 mm ID × 160 mm ID). The column temperature was 40 °C and flow rate was 0.3 mL/min. The eluent conditions were 200 mM HCOOH (A) and CH_3CN (B) using a linear gradient. B% was 60% for 0 to 5 min, 60% to 10% for 5 to 6 min, and 10% for 6 to 20 min. An injection volume of 20 μL containing 0.1μM of each neurotransmitter in water was used for the experiment. The HPLC system was coupled with an electrospray ionization with tandem mass spectrometry (ESI–MS/MS) (MRM positive) detector.

Results

Five neurotransmitters were analyzed using HILICpak VC-50 2D (2.0 mm ID × 150 mm) (Figure 1). Histamine is more basic than the other monoamines analyzed, causing stronger ion exchange interactions between histamine and the packing material causing histamine to elute later.

Conclusions

Shodex HILICpak VC-50 series columns are compatible with MS/MS detection. The polymer-based packing material with diol-like functional groups allows for the detection of monoamine neurotransmitters..

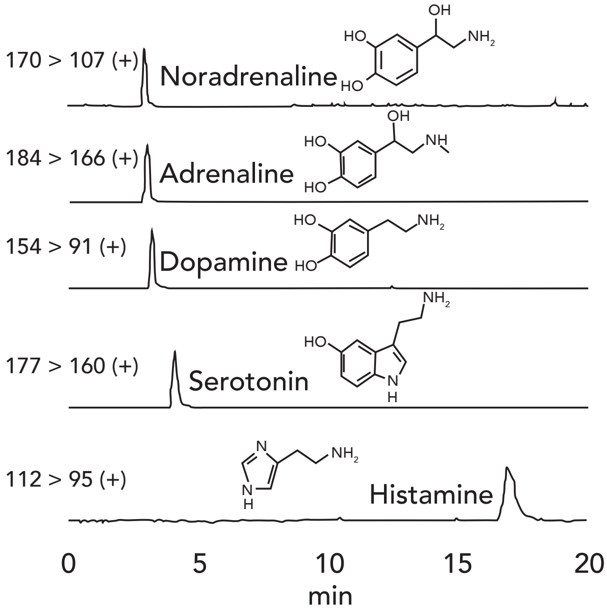

Figure 1: Liquid chromatography with tandem mass spectrometry (LC–MS/MS) analysis of monoamine neurotransmitters using Shodex HILICpak VC-50 2D.

Shodex™
CAPTURE THE ESSENCE

Shodex™/Showa Denko America, Inc.
420 Lexington Avenue Suite 2335A, New York, NY, 10170
Tel. (212) 370-0033 x109, fax (212) 370-4566
Website: www.shodexhplc.com

HAMILTON®

Separation of Common Benzodiazepine Metabolites

Benzodiazepines were first discovered in the 1960's and reached a peak around 1970 with diazepam (Valium). During that time the drug was prescribed for any kind of antihypertensive, analgesic, or psychotropic medications.[1] The overall enthusiasm for the benefits of this class of drug has made a growing trend of addiction more difficult to treat and diagnose. Benzodiazepines became popular due to their safety for the treatment of insomnia and anxiety compared to the preceding sedatives, barbiturates.[2] Benzodiazepines contain a benzene ring fused to a 7-member diazepine ring with variable side chains that can affect potency, duration of action, metabolite activity, and the rate of elimination. Though this class of prescription drugs is considered socially acceptable and generally well tolerated, the addictive effects can be detrimental to life especially when mixed with other drugs. The most commonly mixed drugs with benzodiazepine include over-the-counter cold and flu preparations or ethanol due to the exacerbated effects of mixing.[3] Yet, most metabolite toxicology screens of benzodiazepines are only done for oxazepam-glucuronide. The analysis of the metabolites from benzodiazepine use are of importance in the detection of abuse. Though, the majority of benzodiazepines metabolize to a single compound, oxazolam, other metabolites can be detected by liquid chromatography; Temazepam, α-hydroxyalprazolam, 7-aminoclonazepam, α-hydroxy-midazolam, and the glucuronides of lorazepam, oxazepam, and temazepam (LOT).

In this application note, we examine the chromatography of the aforementioned metabolites from benzodiazepine use. Hamilton's PRP-1, 5 µm, 50 x 4.1 mm HPLC column with the use of ammonium acetate 20 mM buffer to facilitate a run time of less than 10 minutes with good separation between components was used. If a more sensitive detection limit is required, the use of ammonium acetate enables mass spectrometry detection instead of UV used in this application note.

Column Information

Packing Material	P/N
PRP-1, 5 µm	79443

Chromatographic Conditions

Gradient	0.00–2.00 min, 20% B 2.01–10 min, 20–52% B
Temperature	35°C
Injection Volume	5 µL
Detection	UV at 240 nm
Dimensions	50 x 4.1 mm
Eluent A	20 mM CH_3COONH_4
Eluent B	$CH_3CN:CH_3COONH_4$ 20:1
Flow Rate	3.0 mL/min

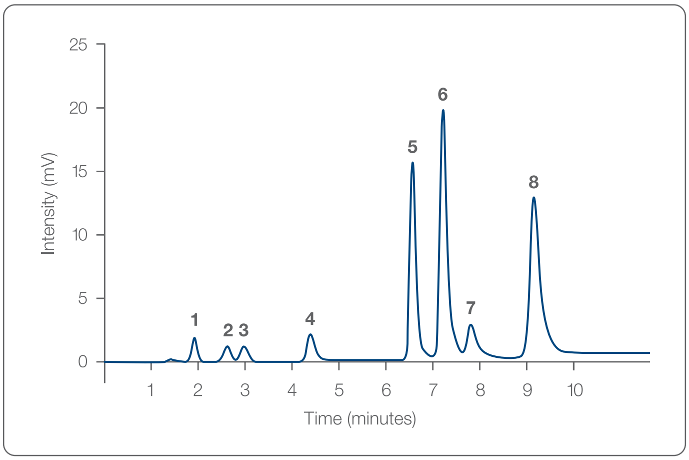

Compounds:

1: Oxazepam Glucuronide
2: Lorazepam Glucuronide
3: Temazepam Glucuronide
4: 7-Aminoclonazepam
5: Alpha-Hydroxyalprazolam
6: Oxazepam
7: Alpha-Hydroxyalprazolam
8: Temazepam

1) *Dodds TJ. Prim Care Companion CNS Disord. 2017. 02:19(2).*

2) *Miller N.S., Gold M.S. Adv Alcohol Subst Abuse. 1990. 8(3–4):67–84.*

3) *Araujo EJF, Rezende-Junior LM, Lima LKF, Silva-Junior MPD, Silva OA, Sousa Neto BP, Almeida AAC, Gutierrez SJC, Tome ADR, Lopes LDS, Ferriera PMP, Lima FDCA. Biomed. Pharmacother. 2018. 103:973–981.*

Author: *Adam L. Moore, PhD, Hamilton Company*

Lit. No. L80104 — 04/2020

Web: www.hamiltoncompany.com
USA: 800-648-5950
Europe: +40-356-635-055
To find a representative in your area, please visit hamiltoncompany.com/contacts.

Hamilton Americas & Pacific Rim
Hamilton Company Inc.
4970 Energy Way
Reno, Nevada 89502 USA
Tel: +1-775-858-3000
Fax: +1-775-856-7259
sales@hamiltoncompany.com

Hamilton Europe, Asia & Africa
Hamilton Central Europe S.R.L.
str. Hamilton no. 2-4
307210 Giarmata, Romania
Tel: +40-356-635-055
Fax: +40-356-635-060
contact.lab.ro@hamilton-ce.com